Cell Stress and Chaperones (2024) 29:235–271
https://doi.org/10.1016/j.cstres.2024.03.001

Comprehensive analysis of human tissues reveals unique expression and localization patterns of HSF1 and HSF2

Jenny Joutsen[1,*] · Jenny C. Pessa[2,3] · Otto Jokelainen[4,5] · Reijo Sironen[4,5] · Jaana M. Hartikainen[4] · Lea Sistonen[2,3,*]

Received: 25 January 2024 / Revised: 29 February 2024 / Accepted: 1 March 2024

Abstract

Heat shock factors (HSFs) are the main transcriptional regulators of the evolutionarily conserved heat shock response. Beyond cell stress, several studies have demonstrated that HSFs also contribute to a vast variety of human pathologies, ranging from metabolic diseases to cancer and neurodegeneration. Despite their evident role in mitigating cellular perturbations, the functions of HSF1 and HSF2 in physiological proteostasis have remained inconclusive. Here, we analyzed a comprehensive selection of paraffin-embedded human tissue samples with immunohistochemistry. We demonstrate that both HSF1 and HSF2 display distinct expression and subcellular localization patterns in benign tissues. HSF1 localizes to the nucleus in all epithelial cell types, whereas nuclear expression of HSF2 was limited to only a few cell types, especially the spermatogonia and the urothelial umbrella cells. We observed a consistent and robust cytoplasmic expression of HSF2 across all studied smooth muscle and endothelial cells, including the smooth muscle cells surrounding the vasculature and the high endothelial venules in lymph nodes. Outstandingly, HSF2 localized specifically at cell–cell adhesion sites in a broad selection of tissue types, such as the cardiac muscle, liver, and epididymis. To the best of our knowledge, this is the first study to systematically describe the expression and localization patterns of HSF1 and HSF2 in benign human tissues. Thus, our work expands the biological landscape of these factors and creates the foundation for the identification of specific roles of HSF1 and HSF2 in normal physiological processes.

Keywords Cell adhesion · Endothelial cells · Formalin-fixed paraffin-embedded (FFPE) · Heat shock factors (HSFs) · Human tissues · Immunohistochemistry

Introduction

Cells in human tissues are constantly exposed to various intracellular and extracellular signals that challenge cellular protein homeostasis or proteostasis. To survive the protein damage, cells employ an evolutionarily well-conserved protective response, termed the heat shock response. The heat shock response is characterized by dramatic transcriptional rewiring that is coordinated by epigenetic enzymes and stress-responsive heat shock factors (HSFs).[1] Upon acute stress, HSFs accumulate in the nucleus and activate the transcription of genes encoding molecular chaperones, including the heat shock proteins (HSPs).[2,3] HSPs assist in the restoration of proteostasis by promoting the refolding, clearance, and disaggregation of misfolded proteins.[4] The human HSF family consists of several members, from which HSF1

* Jenny Joutsen
jenny.joutsen@lapha.fi

* Lea Sistonen
lea.sistonen@abo.fi

1 Department of Pathology, Lapland Central Hospital, Lapland Wellbeing Services County, Rovaniemi, Finland

2 Faculty of Science and Engineering, Cell Biology, Åbo Akademi University, Turku, Finland

3 Turku Bioscience Centre, University of Turku and Åbo Akademi University, Turku, Finland

4 Institute of Clinical Medicine, Clinical Pathology and Forensic Medicine, and Cancer RC, University of Eastern Finland, Kuopio, Finland

5 Department of Clinical Pathology, Kuopio University Hospital, Kuopio, Finland.

Published online: 06 March 2024

and HSF2 are the most extensively studied.[3,5] HSF1 is the predominant regulator of the heat shock response and lack of HSF1 leads to abolished stress resistance and impaired cell survival. In addition to its fundamental role in acute stress, HSF1 is a critical regulator of human pathologies, ranging from metabolic diseases to cancer and neurodegeneration. The functional diversity of HSF1 is reflected by the HSF1-driven gene programs, which differ significantly in their composition between acute stress and disease states.[6–9] In contrast to HSF1, the importance of HSF2 in stress responses and beyond is less understood. HSF2 is not activated by classical acute heat-stress stimuli but acquires DNA-binding capacity in cells undergoing differentiation.[10,11] In the context of stress, HSF2 has been linked with more chronic proteotoxicity caused by elevated temperatures of febrile range,[12] prenatal alcohol exposure,[13] and mild proteasome inhibition.[14,15]

Despite their evident role in cellular perturbations and disease pathogenesis, the function of HSF1 and HSF2 in normal physiological processes has remained largely unexplored. Already the early findings demonstrated that both Hsf1 and Hsf2 are ubiquitously expressed in a wide range of murine tissues, including the brain, skeletal muscle, heart, and testes,[16,17] but how HSFs contribute to normal tissue homeostasis is unknown. Targeted deletion of mouse Hsf1 causes reduced body and organ size and compromises reproduction through placental insufficiency, embryonic lethality, and impaired sperm production.[18–21] Hsf2-deficient mouse models have demonstrated that lack of Hsf2 leads to extensive testicular defects, including reduced testes size, morphologically abnormal seminiferous tubules, and impaired sperm quality.[22–24] Hsf2-null mice display also brain abnormalities caused by the reduced number of radial glia fibers and subsequent neuronal mispositioning.[25] Disruption of both Hsf1 and Hsf2 results in male sterility.[26] However, the HSF-dependent molecular underpinnings of the observed phenotypes require further investigations. Tissues are an elaborate combination of different cell types that, together with the specialized extracellular matrix, maintain the correct structural and functional integrity. Examination of the cell-type specific expression and subcellular localization patterns of HSF1 and HSF2 is mandatory for the identification of HSF-dependent molecular mechanisms maintaining tissue homeostasis.

Here, we used a comprehensive selection of paraffin-embedded archival human tissue material to characterize the distribution of HSF1 and HSF2 in tissues with benign morphology. We show that both HSF1 and HSF2 display cell-type-specific subcellular localization and expression patterns. HSF1 localizes to the nucleus in most, but not all, cell types, whereas HSF2 is predominantly cytoplasmic. Strong nuclear expression of HSF1 was found in all epithelial cell types, including the simple columnar epithelia of the intestine and the luminal epithelia of the breasts. In contrast, nuclear expression of HSF2 was limited to only a few cell types, such as the spermatogonia, the urothelial umbrella cells, and the ciliated cells of the fallopian tubes. Intriguingly, we observed a consistent and strong cytoplasmic expression of HSF2 across all studied smooth muscle tissues, including the vascular smooth muscle cells, the uterine myometrium, and the intestinal muscle layers. Notably, HSF2 was found to specifically localize at cell–cell adhesion sites in a broad selection of tissue types, including the epididymis, cardiac muscle, and the liver. Our findings describing the tissue distribution patterns of HSF1 and HSF2 enable broadening the view of proteostasis regulation from acute stress to benign human physiology.

Results

HSFs mediate cellular responses to protein-damaging stress and are tightly linked with pathological processes, but their relevance in benign human tissues has not been explored. To fill in this gap of knowledge, we investigated the expression and subcellular localization patterns of HSF1 and HSF2 in epithelial, muscular and lymphoid tissues of the circulatory, respiratory, digestive, urinary, and reproductive systems (Figure 1(A)). All examined samples were obtained during routine diagnostic procedures, processed and sectioned. Sequential tissue sections were stained with antibodies against HSF1, HSF2, alpha-smooth muscle actin (SMA), and pan-cytokeratin (CK) (Figure 1(B)). Antibodies against SMA and CK were included as they are commonly used in clinical diagnostics to detect cells with contractile and epithelial properties, respectively. Prior to the analyses, the staining protocols were optimized for the selected antibodies. Breast tissue was used as a positive control for anti-HSF1 antibody (Figure 2(A-a)) and testis as a positive control for anti-HSF2 antibody (Figure 2(A-e)).[27,28] For anti-SMA and anti-CK antibodies, uterine myometrium and breast tissue were used as positive controls, respectively (Figure 2(A-i,k)). Stainings with no primary antibody were used as negative controls (Figure 2(A) middle column a–l). To further verify the specificity and to confirm the compatibility of the selected HSF1 and HSF2 antibodies with human tissue material, we examined HSF1 and HSF2 expression in human osteosarcoma U2OS wild-type, *HSF1* knock-out, and *HSF2* knock-out cells as well as in protein samples extracted from formalin-fixed paraffin-embedded (FFPE) colon muscularis propria and mucosal epithelia

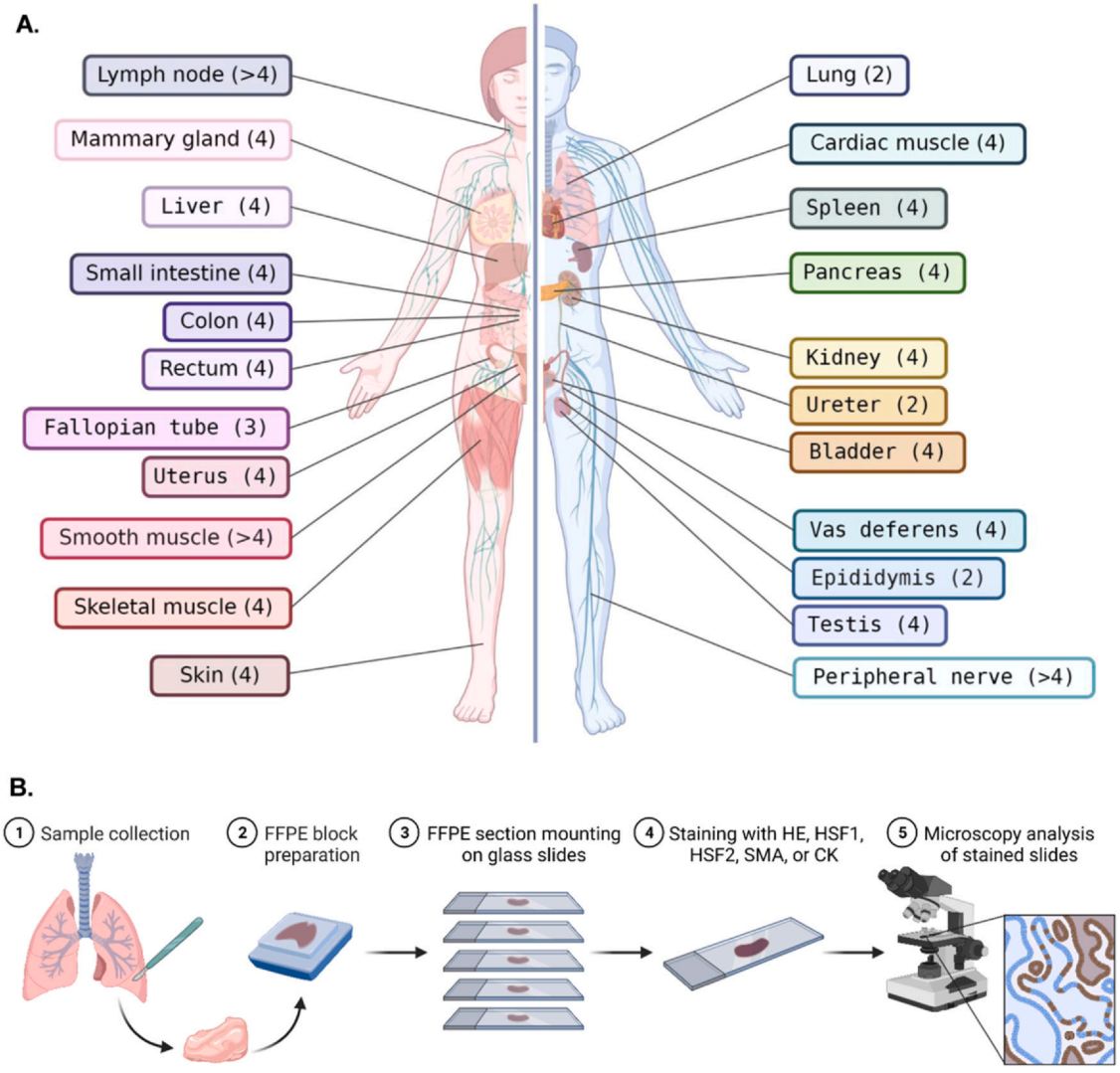

Fig. 1 (A) Schematic presentation of the tissue collection of this study. The number of analyzed samples for each tissue is indicated in brackets. (B) Schematic presentation of the sample examination procedure. Abbreviations used: CK, pan-cytokeratin; FFPE, formalin-fixed paraffin-embedded; HE, hematoxylin and eosin; SMA, alpha-smooth muscle actin. The figure was generated with BioRender.

with immunoblotting. We found that the expression of HSF1 and HSF2 was undetected in their respective knockout cell lines, whereas specific immunoreactive bands of HSF1 and HSF2 were observed in both colonic sample types (Figure 2(B)). These findings confirmed that the selected antibodies were applicable for the detection of HSF1 and HSF2 in human tissue samples. Following optimization, the stainings of sequential tissue sections were analyzed by two independent pathologists, and the scoring results are presented in Table 1.

Skin

The skin is the largest organ of the human body. Its main function is to act as a protective shield against environmental insults, such as mechanical and chemical injuries, and to regulate body temperature. The outermost layer of the skin is called epidermis, and it is a keratinized stratified squamous epithelium. The epidermis is predominantly composed of keratinocytes, but harbors also other cell types, including the neural crest-derived melanocytes that produce melanin and Langerhans cells contributing to immune responses. The dermis lies directly underneath the epidermis and contains, e.g., blood vessels, hair follicles, muscles, sensory neurons, and sweat glands, all embedded in connective tissue. In the skin, HSF1 was strongly expressed in the nucleus and cytoplasm of all examined cell types, including the CK-positive basal and surface keratinocytes (Figure 3(A)), hair follicle epithelial cells, and the ductal epithelium of the sebaceous glands. In contrast, HSF2 displayed only a weak and patchy nuclear expression in basal keratinocytes, whereas, in the surface keratinocytes, a moderate and membranous

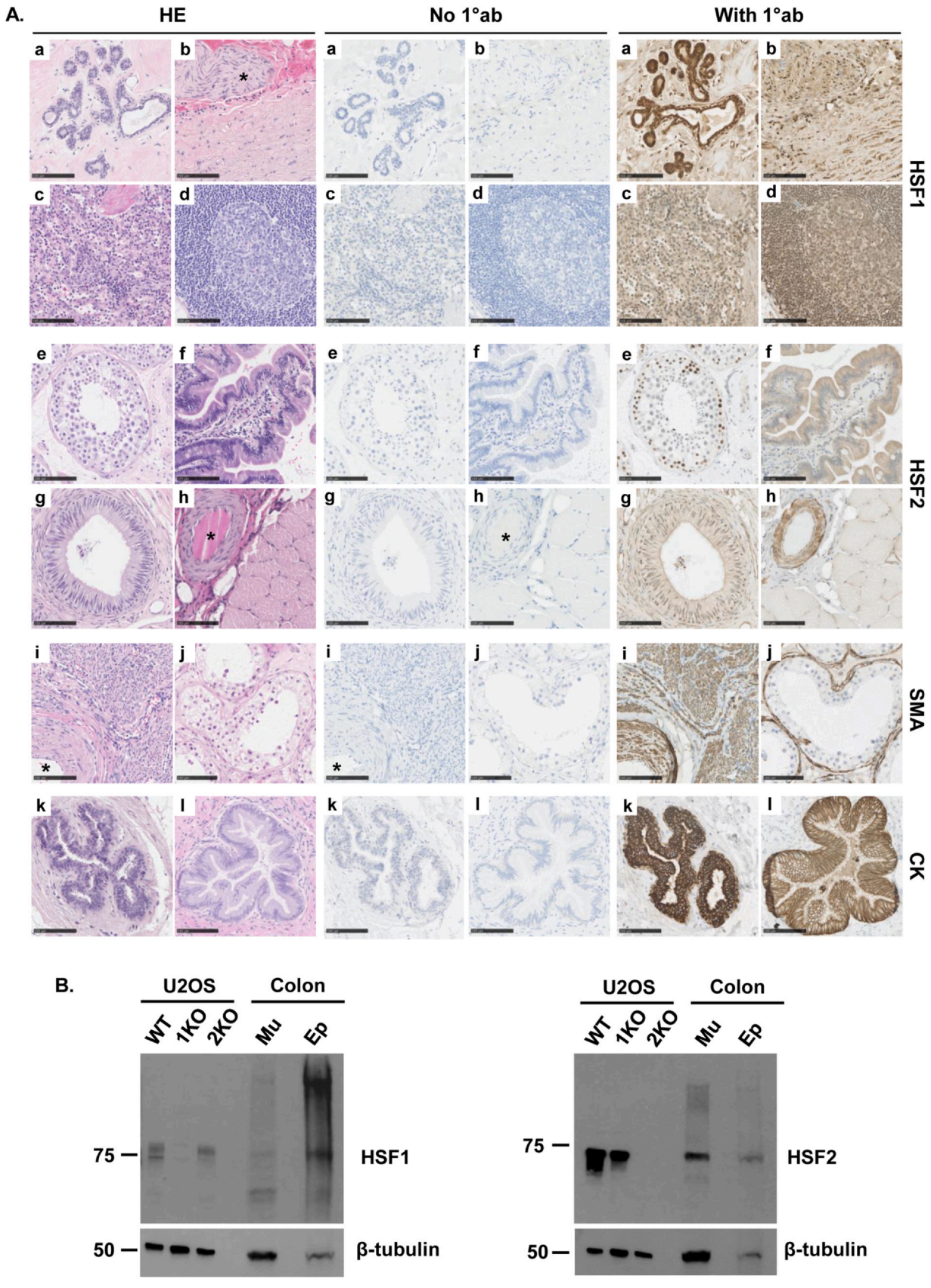
A.
HE
No 1°ab
With 1°ab
HSF1
HSF2
SMA
CK
B.
U2OS
Colon
WT
1KO
2KO
Mu
Ep
75
50
HSF1
β-tubulin
HSF2

Fig. 2 Validation of the antibodies in selected tissues. (A) Stainings with no primary antibody were used as negative controls for antibody specificity. For HSF1 stainings, breast tissue (a), aortic wall and a peripheral nerve (*) (b), red pulp of the spleen (c), and lymphatic follicle (d) are presented. For HSF2 stainings, testis (e), small intestine (f), epididymis (g), and skeletal muscle and an artery (*) (h) are presented. For alpha-smooth muscle actin (SMA), myometrium and an artery (*) (i) and testis (j) are presented. For pan-cytokeratin (CK), breast tissue (k) and endometrial gland (l) are presented. Scale bar 100 μm. (B) Immunoblot analysis of HSF1 and HSF2 in U2OS wild-type (WT), *HSF1* knock-out (1KO), and *HSF2* knock-out (2KO) cells, and in FFPE colon muscularis externa (Mu) and colon mucosal epithelia (Ep). β-tubulin was used as a loading control. Abbreviations used: FFPE, formalin-fixed paraffin-embedded; HE, hematoxylin and eosin.

HSF2 expression was observed (Figure 3(A)). The dermal sweat glands are composed of coiled tubules, which secrete the sweat, and excretory ducts that empty the secretion into hair follicles or to the surface of the skin. The secretory glandular epithelium is surrounded by myoepithelial cells, which function as structural support against hydrostatic pressure.[29] The ductal portion harbors two layers of epithelial cells, the luminal and basal cells, and helps in the reabsorption of ions. In contrast to HSF1, which was expressed in all cell types of the sweat glands (Figure 3(B)), we found that HSF2 is expressed specifically in the cytoplasm of the glandular SMA-positive myoepithelial cells, and also localized at the apical membrane of the ductal luminal cells indicated by the lack of SMA staining (Figure 3(B)). These are the first evidence to demonstrate that HSF1 and HSF2 have clearly divergent expression patterns in intact human tissues. Moreover, these results show that the subcellular localization of HSF2 varies markedly between cells with different phenotypes.

Muscular tissues

The main function of muscular tissues is to provide contractility in the location they reside. The human body harbors three different types of muscle tissue, i.e., skeletal muscle, cardiac muscle, and smooth muscle, which differ in their structural and functional properties. The skeletal muscle tissue consists of elongated multinucleated myotubes that organize as prominently cross-striated myofibers. We analyzed the transverse and longitudinal sections of skeletal muscles and found that HSF1 is strongly expressed in the nuclei and cytoplasm of myofibers, whereas HSF2 expression is rather weak and exclusively cytoplasmic (Figure 4(A) and (B)). The skeletal myofibers can be categorized into two different fiber types based on their contractile and metabolic properties. The slowly twitching type I fibers generate ATP mainly through oxidative metabolism, while the fast twitching type II fibers have a high glycolytic capacity. The proportion of the type I and type II fibers varies between skeletal muscles, and the chessboard-like distribution of fiber types can be identified with additional staining methods, e.g., immunohistochemical typing of myosin heavy chains. Interestingly, the intensity of both HSF1 and HSF2 stainings varied between adjacent myofibers, suggesting that the expression of HSFs might be fiber-type specific (Figure 4(A) and (B)).

The cardiac muscle tissue is composed of branched and striated cardiomyocytes, which contract in a coordinated and rhythmic manner. The rhythmic contraction of the cardiac tissue is ensured by end-to-end coupling of the cardiomyocytes through specialized adhesion complexes, called intercalated discs. The intercalated discs contain a multitude of different cell adhesion contacts, including desmosomes and adherens junctions that provide mechanical strength, and gap junctions and sodium channels that allow the propagation of excitation. By analyzing the transverse and longitudinal sections of cardiac muscle tissue, we observed strong HSF1 and weak HSF2 expression in the nucleus and cytoplasm of cardiomyocytes (Figure 5(A) and (B)). Strikingly, analysis of the longitudinal sections also showed that HSF1 and HSF2 localize specifically to the intercalated discs mediating cell–cell adhesion (Figure 5(B)). This finding is particularly intriguing considering the recent findings linking HSF2 to the maintenance of cell–cell adhesion contacts.[14,30]

The smooth muscle tissue is widely distributed in the human body, as it constitutes the musculature of all internal organs, the digestive system, and the vasculature. In all of these locations, the tissue is composed of spindle-shaped unstriated smooth muscle cells with a single centrally located nucleus. Although the functional role of smooth muscle varies between the organ systems, the involuntary regulation of smooth muscle by the nervous system is mandatory for organismal homeostasis. In the vascular system, the smooth muscle cells surrounding the endothelia are essential for the regulation of blood pressure and flow resistance, but in the urinary tract, they provide elasticity and maintain electrolyte balance by promoting urine flow. In the gastrointestinal tract, the smooth muscle cells ensure the propulsion of food, whereas the uterine smooth muscle generates pregnancy-associated contractions. As examples of smooth muscle tissues, we present here the smooth muscle layer of the bladder (Figure 6(A)), the vascular smooth muscle cells surrounding an artery (Figure 6(A)), and the outer longitudinal muscle layer of the colon (Figure 6(B)). In these samples, HSF1 was strongly expressed both in the nucleus and cytoplasm of

Table 1
Expression and subcellular localization of HSF1 and HSF2 was evaluated by two independent pathologists (1 = weak, 2 = moderate, 3 = strong).

Cell type	Organ(s)	HSF1 intensity	HSF1 localization	HSF2 intensity	HSF2 localization	Figure
Basal keratinocytes	Epidermis	3+	Cytoplasmic & Nuclear	1+ (Patchy)	Nuclear	3
Surface keratinocytes	Epidermis	3+	Cytoplasmic & Nuclear	2+	Membranous	3
Sweat duct epithelium	Dermis	3+	Cytoplasmic & Nuclear	1+	Membranous	3
Sweat duct myoepithelial cells	Dermis	3+	Cytoplasmic & Nuclear	3+	Cytoplasmic	3
Hair follicle epithelial cells	Dermis	3+	Cytoplasmic & Nuclear	1+ (Patchy)	Nuclear	3
Sebaceous gland epithelial cells	Dermis	3+	Cytoplasmic & Nuclear	1+ (Patchy)	Nuclear	-
Skeletal muscle cell	All examined	3+	Cytoplasmic & Nuclear	1+	Cytoplasmic	4
Cardiomyocyte	Heart	3+	Cytoplasmic & Nuclear	1+	Cytoplasmic	5
Cardiomyocyte (intercalated discs)	Heart	2+	-	2+	-	5
Smooth muscle cell	All examined	3+	Cytoplasmic & Nuclear	2+	Cytoplasmic	6, 19, 21
Vessel wall muscle cell	All examined	3+	Cytoplasmic & Nuclear	2+	Cytoplasmic	6
Endothelial cell	All examined	3+	Cytoplasmic & Nuclear	2+	Cytoplasmic	6, 8, 9, 10
Ganglion cells	Intestine wall	3+	Cytoplasmic & Nuclear	3+	Cytoplasmic	7
Endoneurium Schwann cells	Peripheral nerves	3+	Cytoplasmic & Nuclear	2+	Cytoplasmic	7
Perineurium	Peripheral nerves	3+	Cytoplasmic & Nuclear	0	-	7
Lymphocytes	Multiple organ systems	2+ (Patchy)	Nuclear	0	-	8, 9
Plasma cells	Lymph nodes	3+	Cytoplasmic	1+	Cytoplasmic	9
Macrophages	Lymph nodes, lungs	3+	Cytoplasmic & Nuclear	0	-	9, 10
Enterocyte	Small intestine	3+	Cytoplasmic & Nuclear	2+	Cytoplasmic	11
Enterocyte	Colon, rectum	3+	Cytoplasmic & Nuclear	2+	Cytoplasmic	12, 13
Langerhans islet cells	Pancreas	3+	Cytoplasmic & Nuclear	1+	Cytoplasmic	14
Acinar cell	Pancreas	2+	Cytoplasmic & Nuclear	0	-	14
Hepatocytes	Liver	2+	Cytoplasmic	0	-	15
Liver sinusoidal cell	Liver	3+	Nuclear	0	-	15
Biliary epithelium	Liver	2+	Cytoplasmic & Nuclear	2+	Cytoplasmic	15
Biliary canaliculi	Liver	0	-	1+	-	15
Epithelial cell (prox. conv. tubule)	Kidney	1+	Cytoplasmic & Nuclear	1+	Cytoplasmic	16
Epithelial cell (dist. conv. tubule)	Kidney	3+	Cytoplasmic & Nuclear	2+	Cytoplasmic	16
Epithelial cell (collecting duct)	Kidney	2+	Cytoplasmic & Nuclear	1+	Cytoplasmic	16
Urothelium	Pelvis, bladder	3+	Cytoplasmic & Nuclear	2+	Cytoplasmic	17
Urothelium (umbrella cells)	Pelvis, bladder	3+	Cytoplasmic & Nuclear	2+	Nuclear	17
Spermatogonia	Testis	3+	Nuclear	3+	Nuclear	18
Epithelial cells	Epididymis	3+	Cytoplasmic & Nuclear	1+	Membranous	19
Vas deferens epithelial cell	Vas deferens	3+	Cytoplasmic & Nuclear	1+	Membrane	19
Acinar cell	Breast	2+	Cytoplasmic & Nuclear	1+	Cytoplasmic	20
Myoepithelial cells	Breast	3+	Cytoplasmic & Nuclear	2+	Cytoplasmic	20
Breast duct epithelium	Breast	3+	Cytoplasmic & Nuclear	1+	Cytoplasmic	20
Endometrial epithelial cell	Endometrium	3+	Cytoplasmic & Nuclear	2+	Cytoplasmic	21
Serous epithelial cell	Uterine tube	3+	Cytoplasmic & Nuclear	1+	Cytoplasmic	22
Intercalated cell	Uterine tube	3+	Cytoplasmic & Nuclear	1+	Nuclear	22
Fibroblast	All examined	3+	Cytoplasmic & Nuclear	1+	Cytoplasmic	-
Endocervical epithelial cell	Endocervix	3+	Cytoplasmic & Nuclear	2+	Cytoplasmic	-
Mesothelial cell	Abdominal cavity	3+	Cytoplasmic & Nuclear	2+	Cytoplasmic & Nuclear	-
Paratesticular epithelial cell	Paratestis	3+	Nuclear	1+	Membrane	-
Schwann cells	Multiple organ systems	3+	Cytoplasmic & Nuclear	1+	Cytoplasmic	-
Adipocytes	Multiple organ systems	3+	Nuclear	0	-	-

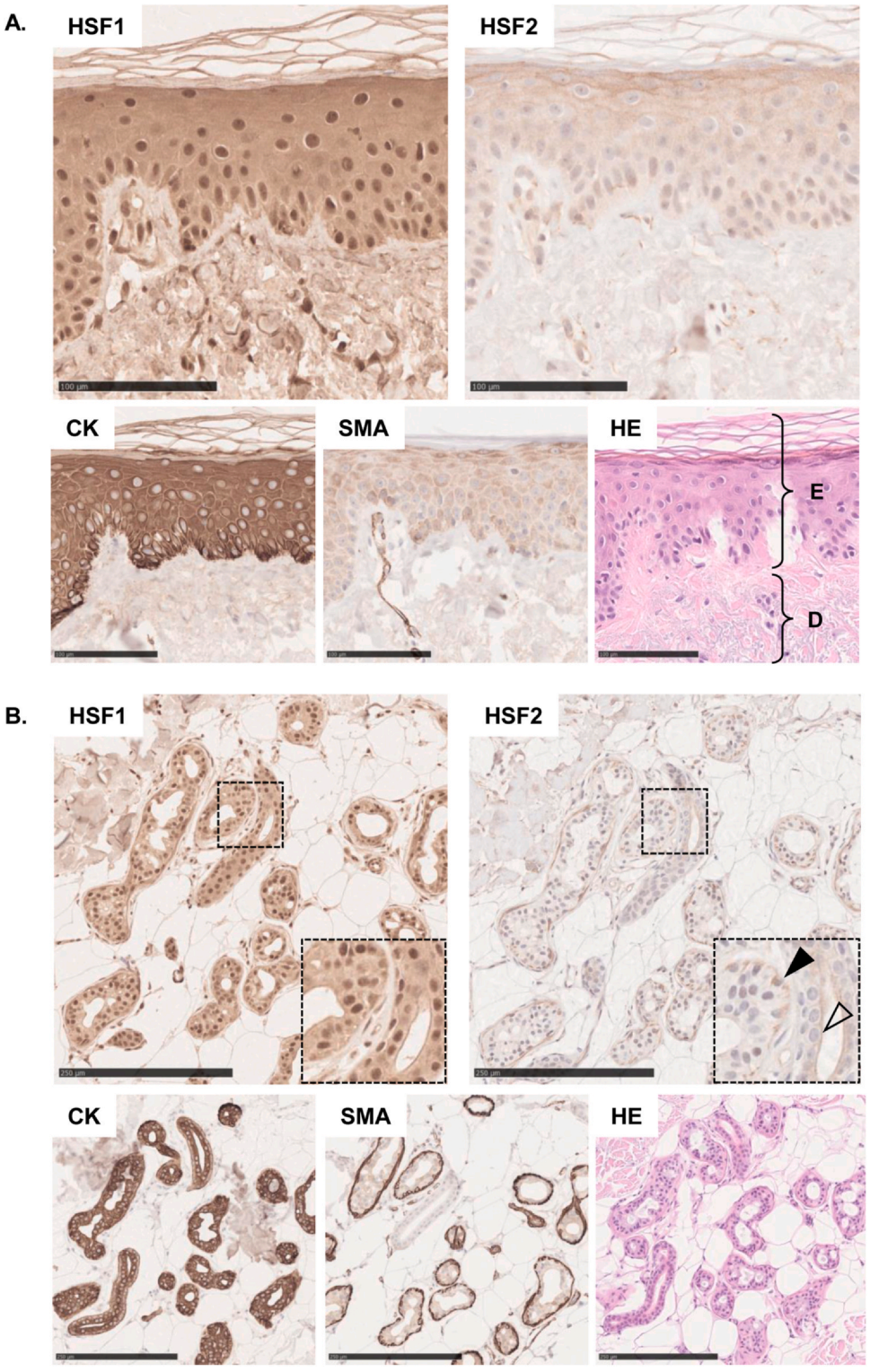

Fig. 3 Cross-section of the skin. (A) HSF1 is strongly expressed in the nucleus and cytoplasm of all examined cell types including the CK-positive basal and surface keratinocytes. HSF2 expression in basal keratinocytes is weak and patchy. In the surface keratinocytes, moderate and membranous HSF2 expression is observed. Scale bar 100 μm. (B) Dermal sweat gland. HSF1 is expressed in all cell types of the sweat glands. HSF2 localizes specifically in the cytoplasm of SMA-positive myoepithelial cells and at the apical membrane of the ductal luminal cells indicated by lack of SMA staining. In the HSF2 inset, the arrowhead indicates cytoplasmic HSF2 expression in the myoepithelial cells of the secretory ducts. The open arrowhead indicates HSF2 localization to apical plasma membrane in the luminal cells of the excretory duct. Scale bar 250 μm. Abbreviations used: CK, pan-cytokeratin; D, dermis; E, epidermis; HE, hematoxylin and eosin; SMA, alpha-smooth muscle actin.

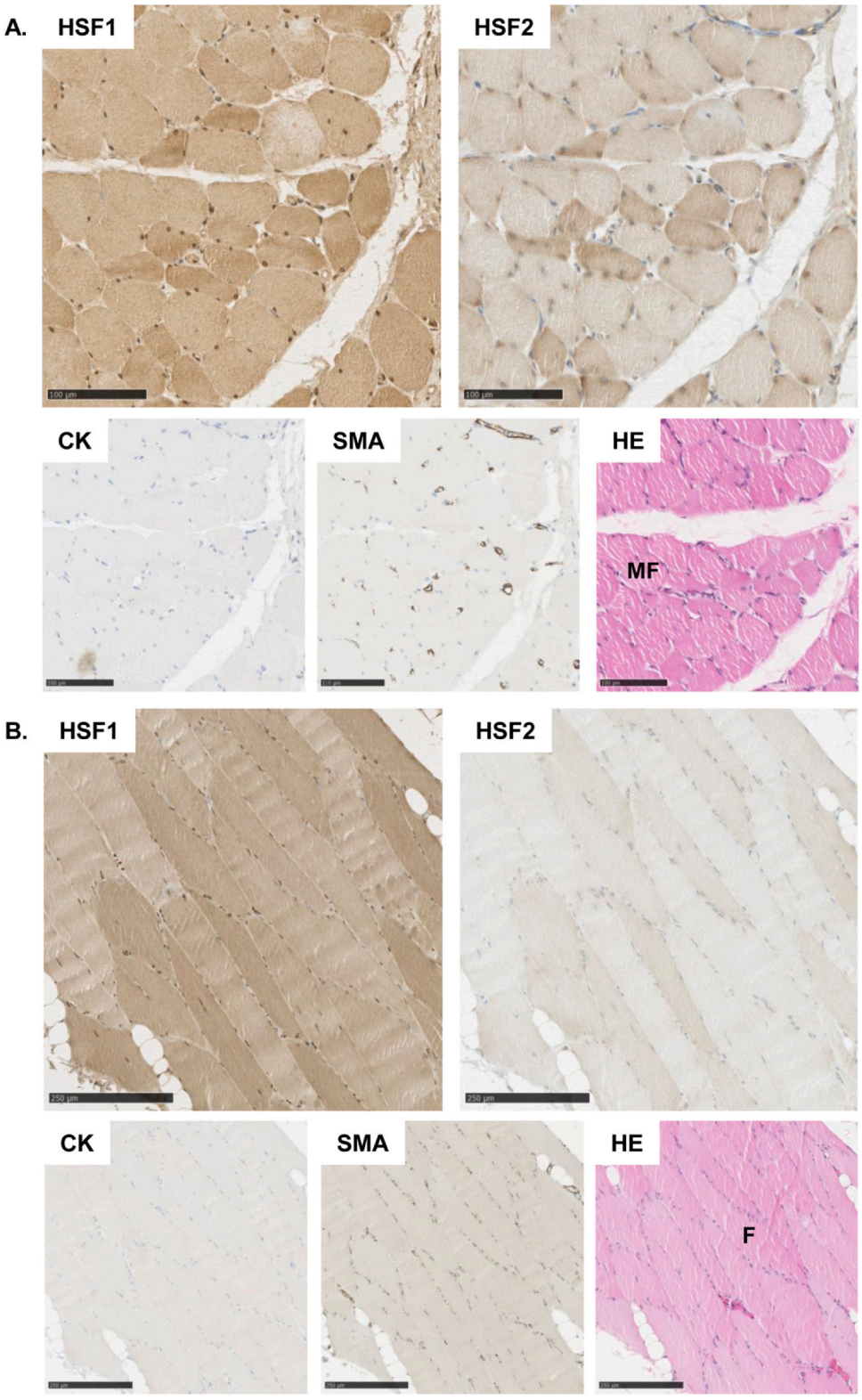

Fig. 4 Cross-section of skeletal muscle tissue. HSF1 is strongly expressed in the nuclei and cytoplasm of myofibers, while HSF2 expression is weak and exclusively cytoplasmic. The intensity of both HSF1 and HSF2 stainings varies between adjacent myofibers. (A) Transverse section. Scale bar 100 μm. (B) Longitudinal section. Scale bar 250 μm. Abbreviations used: CK, pan-cytokeratin; F, muscle fascicle; HE, hematoxylin and eosin; MF, muscle fiber; SMA, alpha-smooth muscle actin.

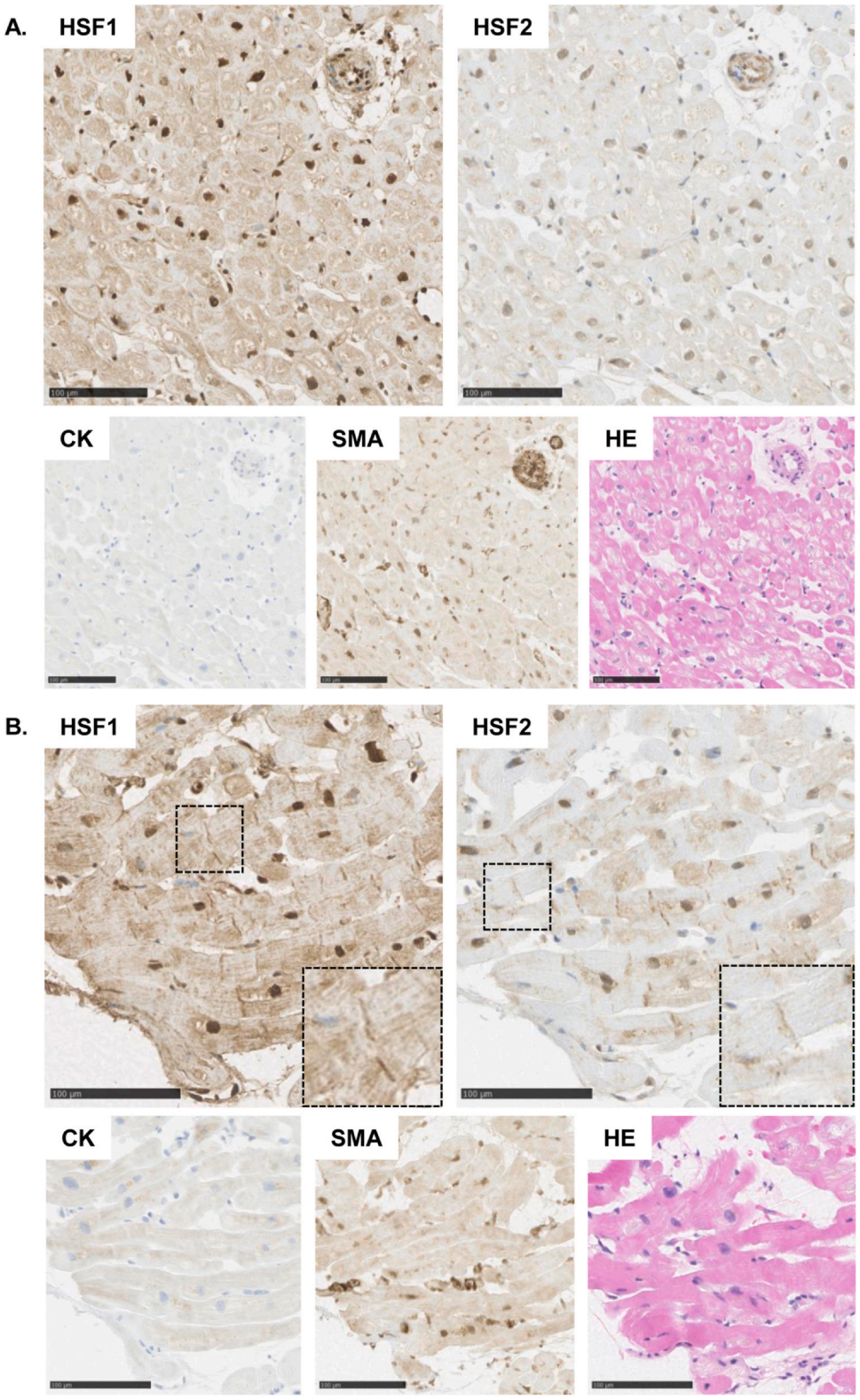

Fig. 5 Cross-section of cardiac muscle tissue. (A) Transverse section of cardiac tissue. Strong HSF1 and weak HSF2 expression is observed in the nucleus and cytoplasm of cardiomyocytes. (B) Longitudinal section of cardiac tissue. HSF1 and HSF2 localize specifically to the intercalated discs connecting cardiomyocytes. The HSF1 and HSF2 insets highlight the localization to intercalated discs. Scale bar 100 μm. Abbreviations used: CK, pan-cytokeratin; HE, hematoxylin and eosin; SMA, alpha-smooth muscle actin.

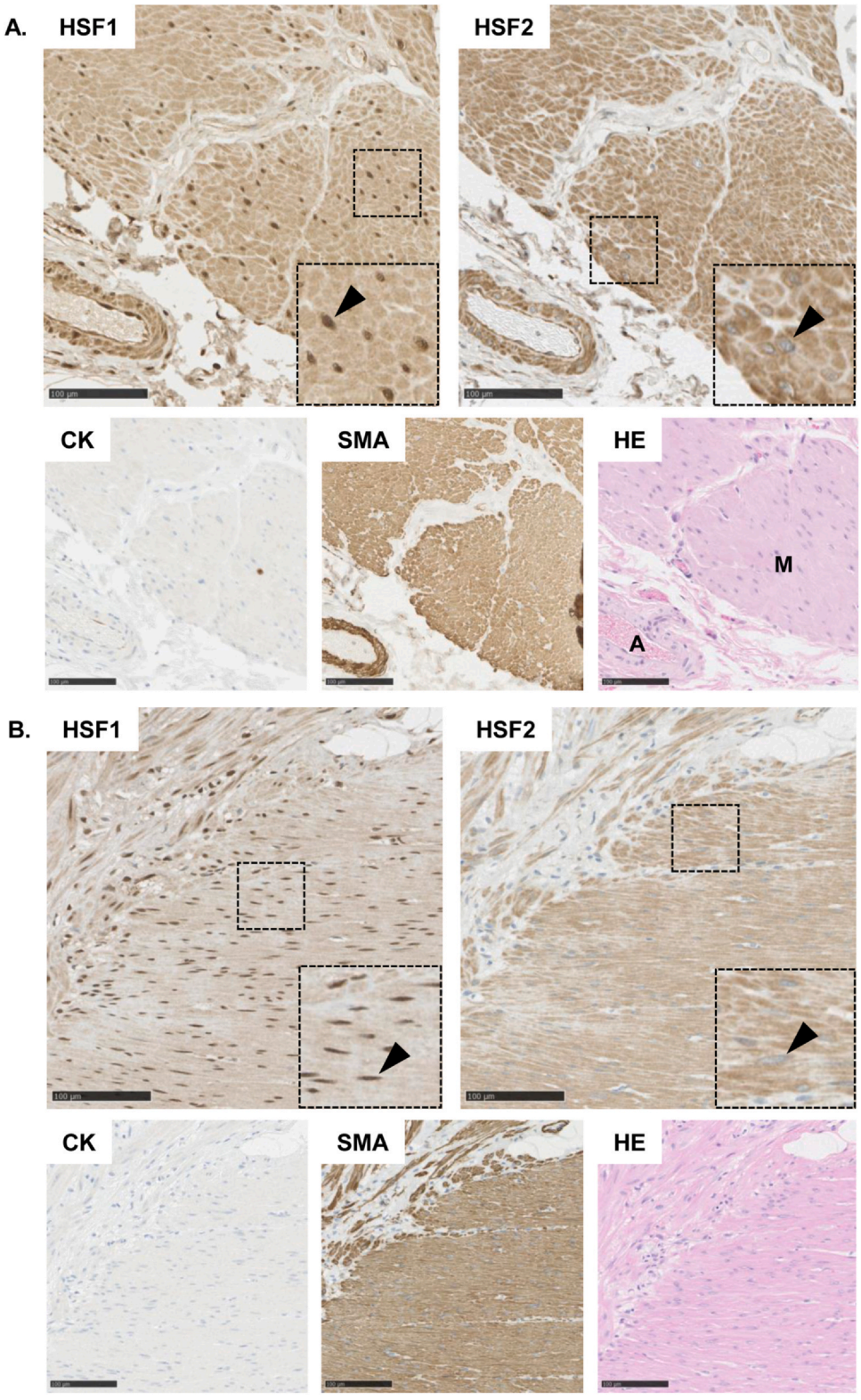

Fig. 6 Cross-section of smooth muscle tissue. HSF1 is strongly expressed both in the nucleus and cytoplasm of the smooth muscle cells. HSF2 expression is moderate and it localizes exclusively in the cytoplasm. (A) Urinary bladder. In the HSF1 and HSF2 insets, the arrowhead indicates the nucleus of a smooth muscle cell. Scale bar 100 μm. (B) Muscularis externa of the colon. In the HSF1 and HSF2 insets, the arrowhead indicates the nucleus of a smooth muscle cell. Scale bar 100 μm. Abbreviations used: A, artery; CK, pan-cytokeratin; HE, hematoxylin and eosin; M, muscle layer; SMA, alpha-smooth muscle actin.

smooth muscle cells (Figure 6(A) and (B)). HSF2 was also moderately expressed in smooth cells, but localized exclusively in the cytoplasm (Figure 6(A) and (B)). Strikingly, an examination of other smooth muscle tissues included in our sample set revealed that the HSF2 signal is detected in the cytoplasm of all smooth muscle cells. To the best of our knowledge, this is the first study to describe a consistent and comprehensive cytoplasmic localization of HSF2 in smooth muscle cells. Due to the consistency of our findings, we compared our results to the HSF1 and HSF2 tissue expression patterns presented in the Human Protein Atlas (HPA, www.proteinatlas.org, 2023). In support of our results, HSF1 displays prominent nuclear and cytoplasmic expression also in smooth muscle cells samples of the HPA tissue collection (e.g., Gallbladder, ID2446, Uterus, ID2225), while the expression of HSF2 is moderate and solely cytoplasmic (e.g., Prostate, ID2932; Urinary bladder, ID3184; Endometrium, ID1488). Altogether, these results describe a prominent expression pattern of HSFs in smooth muscle tissues and indicate HSFs as putative contributors in smooth muscle tissue homeostasis.

Peripheral nerves

The human nervous system is a complex network of functionally divergent neurons that can be anatomically divided into the central nervous system (CNS) and the peripheral nervous system. The CNS comprises the brain and the spinal cord, while the peripheral nervous system includes nerve fibers that provide organ innervation. Peripheral nerve fibers are composed of axons and dendrites, which in myelinated fibers are surrounded by a myelin sheath derived from Schwann cells. The nuclei of Schwann cells are visible in the cross-section of peripheral nerves. We found that HSF1 is strongly expressed in the nucleus and cytoplasm of most but not all Schwann cells and in the fibroblast-like perineural cells encapsulating the nerve fascicle (Figure 7(A)). In contrast, HSF2 was only weakly expressed in the cytoplasm of some Schwann cells and no signal of HSF2 was observed in the perineurium (Figure 7(A)).

The innervation of the intestinal wall is covered by nerve plexuses that harbor sympathetic and parasympathetic fibers, satellite cells, Schwann cells, and ganglion cells that innervate the intestinal smooth muscle, the blood vessels, and the intestinal glands. Myenteric plexus is the major nerve supply responsible for intestinal movement and it is located between the circular and longitudinal layers of the intestinal muscularis externa. The ganglion cells within the myenteric plexus are large multipolar neurons with a prominent nucleolus. By investigating the myenteric plexus in our gastrointestinal tissue samples, we found that HSF1 is strongly expressed in the nucleus and cytoplasm of ganglion and satellite cells, whereas HSF2 is expressed only in the ganglion cells and localizes specifically to the cytoplasm (Figure 7(B)).

Lymphatic system

The main function of the lymphatic system is to maintain the body's fluid balance and regulate immune responses. The lymphatic system is built by a network of lymphatic vessels, lymphatic organs and tissues, and the lymph. The generation of lymphocytes from immature progenitors occurs in primary lymphatic organs, the bone marrow, and the thymus. Mature lymphocytes are stored in secondary lymphatic organs, the spleen, and the lymph nodes, which serve as platforms for the initiation of the adaptive immune response. We investigated the expression and subcellular localization of HSF1 and HSF2 in tissue samples from the spleen and lymph nodes.

The spleen is an encapsulated organ that can be structurally divided into splenic pulps: the white pulp and the red pulp. The white pulp entails the lymphatic tissue that is arranged as periarterial lymphoid sheaths composed of mature T-cells and as splenic follicles containing B-cells, macrophages, and dendritic cells. The major components of the red pulp are the splenic cords and the venous sinuses, which together mediate the filtering and recycling of red blood cells. The venous sinuses are formed by endothelial cells with nuclei bulging into the lumen of the sinus. We detected a moderate nuclear expression of HSF1 in all lymphocytes present in the white pulp (Figure 8(A)). No signal of HSF2 was detected in splenic lymphocytes (Figure 8(A)). Both HSF1 and HSF2 signals were observed in the sinusoidal endothelial cells of the red pulp (Figure 8(B)). In these cells, HSF1 localized to both the nucleus and cytoplasm, which is in sharp contrast to HSF2 that was found exclusively in the cytoplasm of the endothelial cells (Figure 8(B)).

Lymph nodes are small bean-shaped organs that arrange along the lymphatic vessels. The primary function of lymph nodes is to filter lymph for the identification of infectious agents. Each lymph node is covered by a connective tissue capsule that extends as trabeculae into the substance of the tissue. The parenchyma of the lymph node is classified into three regions: the cortex that contains B-cell lymphoid follicles, the paracortex containing T-cells, and the medulla harboring medullary cords and sinuses. A secondary lymphoid follicle is composed of a germinal center that is surrounded by a mantle zone and diffuse lymphatic tissue. In line with our findings from the spleen, HSF1 was strongly expressed in the nucleus of the lymphocytes of

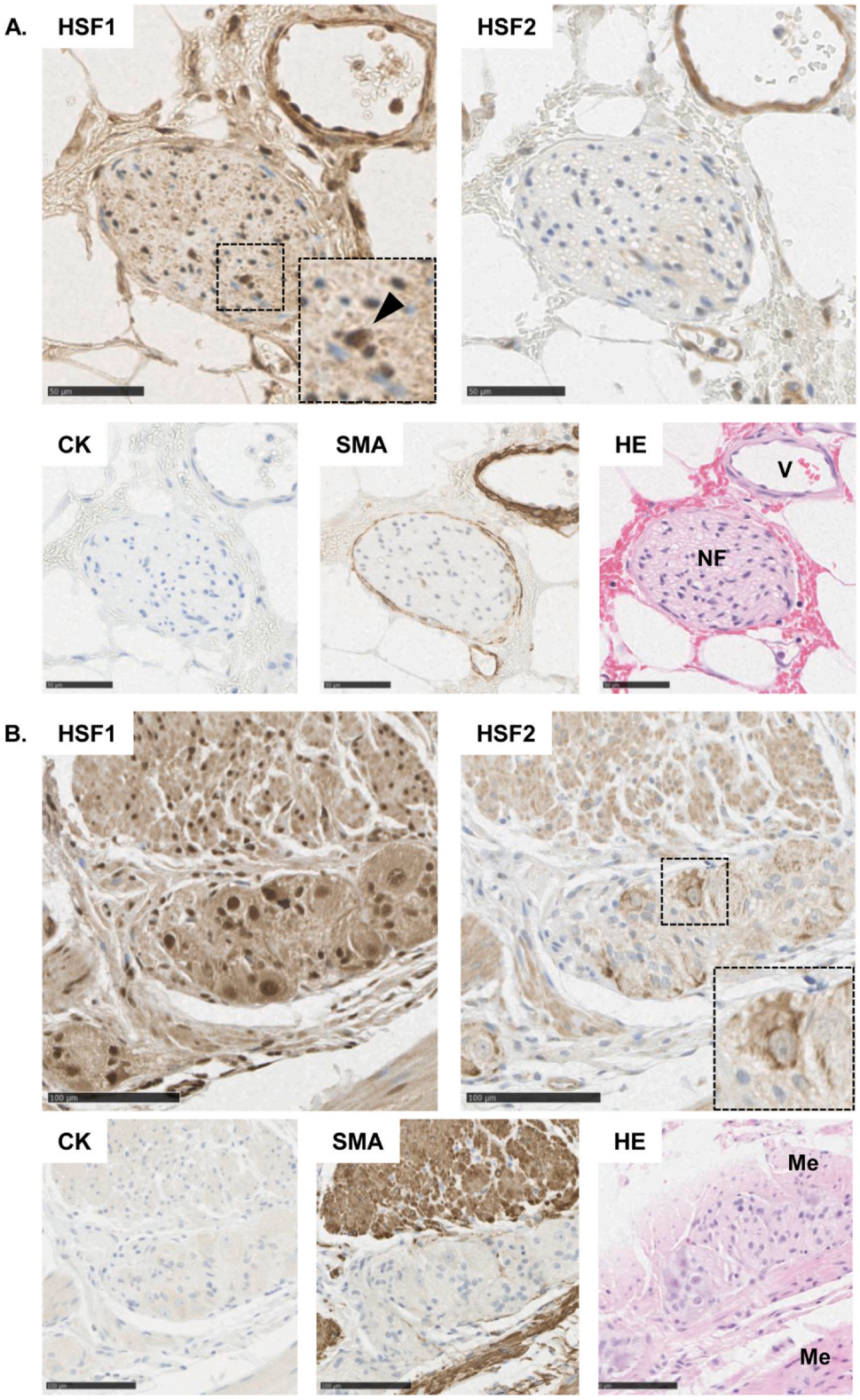

Fig. 7 Cross-section of peripheral nerves. (A) Nerve fiber adjacent to spleen. HSF1 is strongly expressed in the nucleus of most but not all Schwann cells and in the fibroblast-like perineural cells encapsulating the nerve fascicle. In the HSF1 inset, the arrowhead indicates an HSF1-positive Schwann cell nucleus. Scale bar 50 μm. (B) Myenteric plexus in the intestinal wall. HSF1 is strongly expressed in the nucleus and cytoplasm of ganglion and satellite cells, while HSF2 is expressed only in the ganglion cells and localizes to the cytoplasm. The HSF2 inset highlights the cytoplasmic expression of HSF2 in the ganglion cells. Scale bar 100 μm. Abbreviations used: CK, pan-cytokeratin; HE, hematoxylin and eosin; Me, muscularis externa; NF, nerve fiber; SMA, alpha-smooth muscle actin; V, vein.

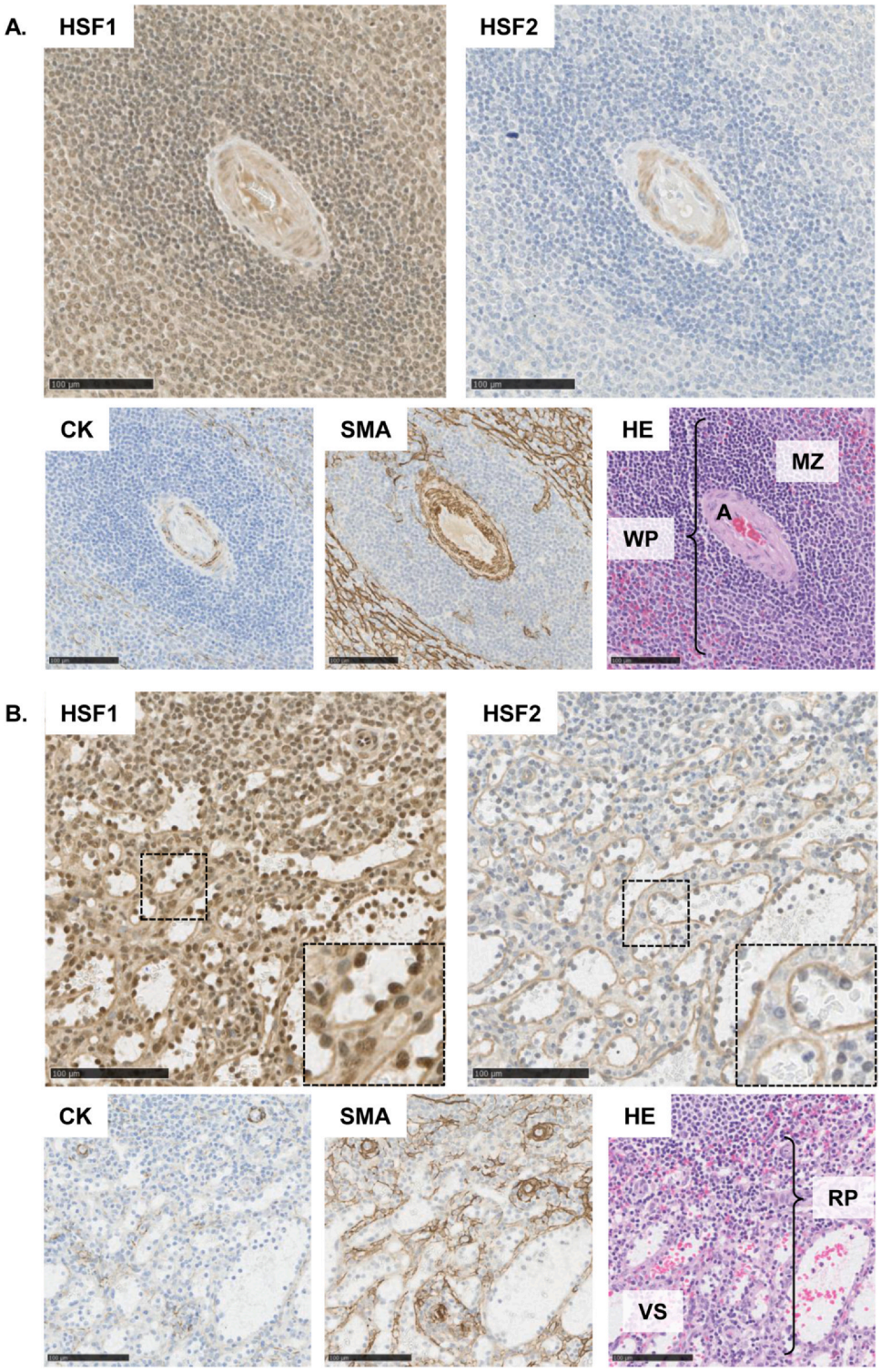

Fig. 8 Cross-section of the spleen. (A) Moderate nuclear expression of HSF1 is detected in all lymphocytes present in the white pulp. No signal of HSF2 is detected in splenic lymphocytes. (B) HSF1 and HSF2 signals are detected in the sinusoidal endothelial cells of the red pulp. The HSF1 and HSF2 insets highlight sinusoidal endothelial cells. Scale bar 100 μm. Abbreviations used: A, central arteriole; CK, pan-cytokeratin; HE, hematoxylin and eosin; MZ, marginal zone; RP, red pulp; SMA, alpha-smooth muscle actin; VS, vascular sinusoids; WP, white pulp.

lymphatic follicles, whereas no lymphocytic signal of HSF2 could be detected (Figure 9(A)). The major gateways for lymphocyte entry into lymph nodes are specialized post-capillary vessels termed high endothelial venules (HEVs). The HEVs reside exclusively in the cortical region of lymph nodes and are characterized by cuboidal endothelial cells that differ morphologically from the flat endothelial cells lining other types of vessels. We found that both HSF1 and HSF2 were expressed in the endothelial cells of the HEVs (Figure 9(B)). Similarly to the flat splenic endothelial cells, HSF1 localized in both the nucleus and cytoplasm of the HEV endothelial cells, and HSF2 was localized only in the cytoplasm. Of note, a full analysis of our tissue collection revealed that HSF1 and HSF2 are, in fact, expressed in all studied endothelial cells in a manner similar to the examples from lymphoid tissues. Together with our findings demonstrating HSF1 and HSF2 signals in vascular smooth muscle cells (Figure 6(A)), these results show that HSFs are strongly expressed in the key cell types of human vasculature.

Lung

The functional unit of the lungs includes respiratory bronchioles, alveolar ducts, alveolar sacs, and alveoli. The respiratory bronchioles are lined by ciliated simple columnar respiratory epithelium, and the wall contains an incomplete layer of smooth muscle fibers embedded in connective tissue. We found that HSF1 is strongly expressed in the nucleus and cytoplasm of the CK-positive respiratory epithelial cells (Figure 10(A)). HSF2 was not found in the respiratory epithelia, but it displayed moderate expression in the cytoplasm of the SMA-positive smooth muscle cells of respiratory bronchioles and arteries (Figure 10(A)). Pulmonary gas exchanges occur in the alveoli, which are cup-shaped cavities surrounded by a network of small capillaries. There are three major types of alveolar cells, type I and type II pneumocytes and the alveolar macrophages. Type I cells are extremely thin squamous epithelial cells that mediate the gas exchange between the blood and the alveoli. Type II cells are more cuboidal and responsible for the secretion of pulmonary surfactant. Alveolar macrophages reside in the alveolar cavity and are often called dust cells due to their engulfment of foreign particles. The used antibodies cannot reliably distinguish between the type I and type II pneumocytes. However, HSF1 was strongly expressed in the nucleus and cytoplasm of the CK-positive epithelial cells lining the alveoli (Figure 10(A) and (B)). Also, the intra-alveolar macrophages displayed strong expression of HSF1, which surprisingly was found to localize only in the cytoplasm of individual cells (Figure 10(B)). HSF2 was undetectable in alveolar epithelial cells (Figure 10(A) and (B)), but a moderate cytoplasmic expression in alveolar macrophages and in the endothelial cells forming the pulmonary capillaries was observed (Figure 10(B)).

Intestine

The intestine composes the lower part of the gastrointestinal tract and consists of the small intestine and the large intestine. The small intestine is further divided into the sections of the duodenum, jejunum, and ileum, which function together in the absorption of digestive products. Although the sections differ to some extent in their histological structure, the whole small intestinal mucosa is covered by simple columnar epithelium consisting of a few major cell types. The enterocytes form the microvilli-covered brush border and are thus the main absorptive cell type. The Goblet cells are responsible for the production of mucus, whereas the enteroendocrine cells regulate digestive functions through peptide hormones. In our samples of the small intestine, HSF1 was strongly expressed in the nucleus and cytoplasm of the CK-positive enterocytes but localized only to the cytoplasm of individual Goblet cells (Figure 11). HSF2 displayed a moderate cytoplasmic expression pattern in the enterocytes with a possible concentration on the apical junctional complex underlining the microvilli. In support of our findings, cytoplasmic and membranous HSF2 localization is reported also in the small intestinal samples of the HPA (ID3852, ID2450, and ID1879). Importantly, the samples of HPA show localization of HSF2 at the epithelial apical junctional complex that serves as the foundation for the intestinal barrier.

The large intestine is subdivided into cecum, colon, rectum, and the anal canal, and it functions in the absorption of water and salts. Similarly to the small intestine, the wall of the large intestine is lined by simple columnar epithelium with enterocytes, Goblet cells, and enteroendocrine cells. In the colon, the epithelium invaginates into colonic crypts with intestinal stem cells localized in the bottom of the crypts. By analyzing the longitudinal and transverse sections of the crypts, we found that HSF1 is present in the nucleus and cytoplasm of the colonic enterocytes, but localizes only to the cytoplasm of the Goblet cells (Figure 12(A) and (B)). Weak expression of HSF2 was detected in the cytoplasm of the enterocytes and in the SMA-positive smooth muscle cells forming the muscle fibers of intestinal muscularis mucosa (Figure 12(A) and (B)). The microanatomy of the rectum is similar to the rest of the intestinal tract. The rectal enterocytes showed strong expression of HSF1 in the nucleus and cytoplasm, whereas only moderate expression of HSF2 was observed in the cytoplasm (Figure 13). In line with our results from small

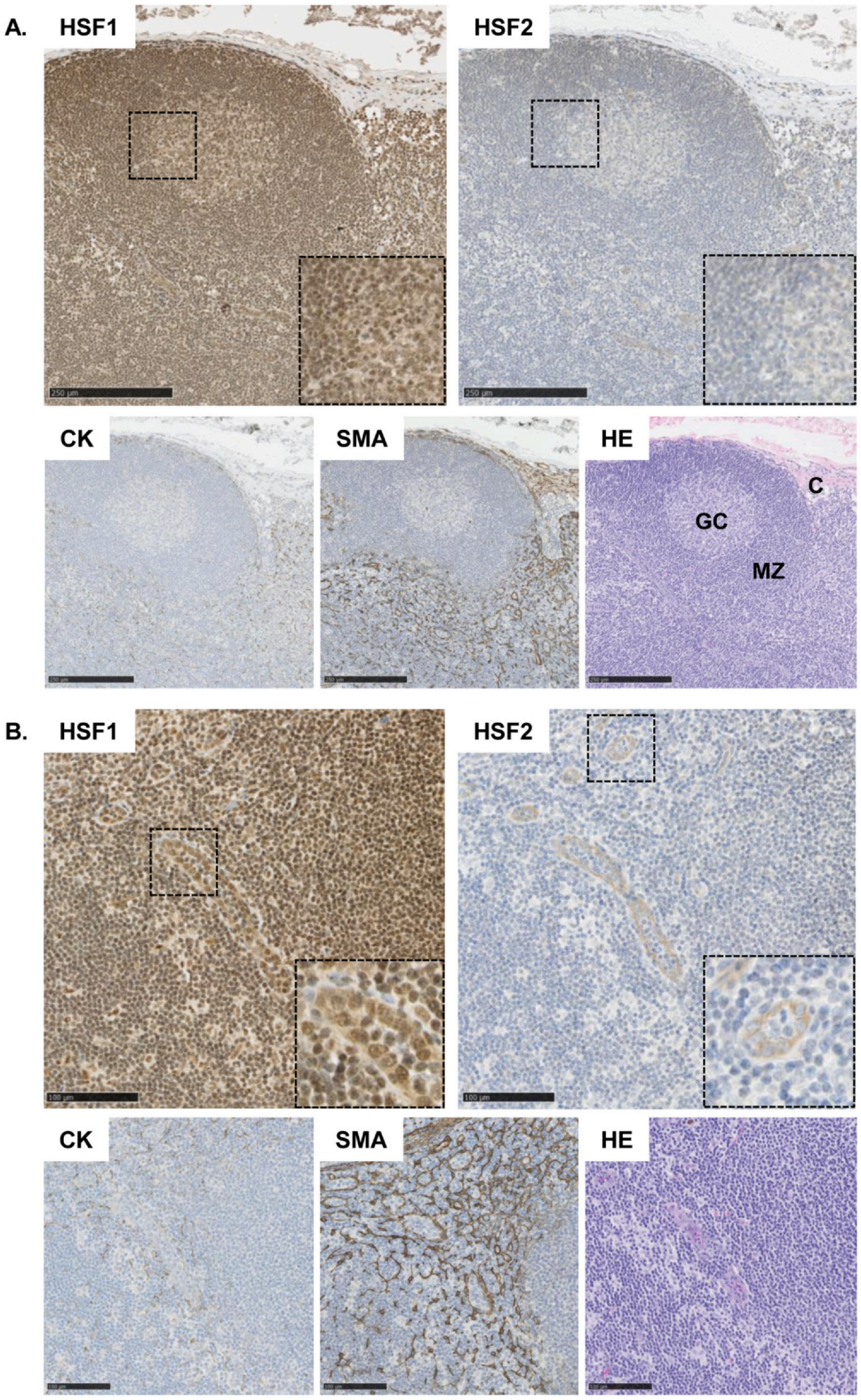

Fig. 9 Cross-section of a lymph node. (A) Lymphatic follicle at the outer cortex of a lymph node. HSF1, but not HSF2, is strongly expressed in the nucleus of lymphocytes of lymphatic follicles. (B) High endothelial postcapillary venules. Both HSF1 and HSF2 are expressed in the endothelial cells, where HSF1 localizes in the nucleus and the cytoplasm and HSF2 in the cytoplasm. The HSF1 and HSF2 insets highlight the endothelial cells of the postcapillary venules. Scale bar 250 μm. Abbreviations used: C, capsule; CK, pan-cytokeratin; GC, germinal center; HE, hematoxylin and eosin; MZ, mantel zone; SMA, alpha-smooth muscle actin.

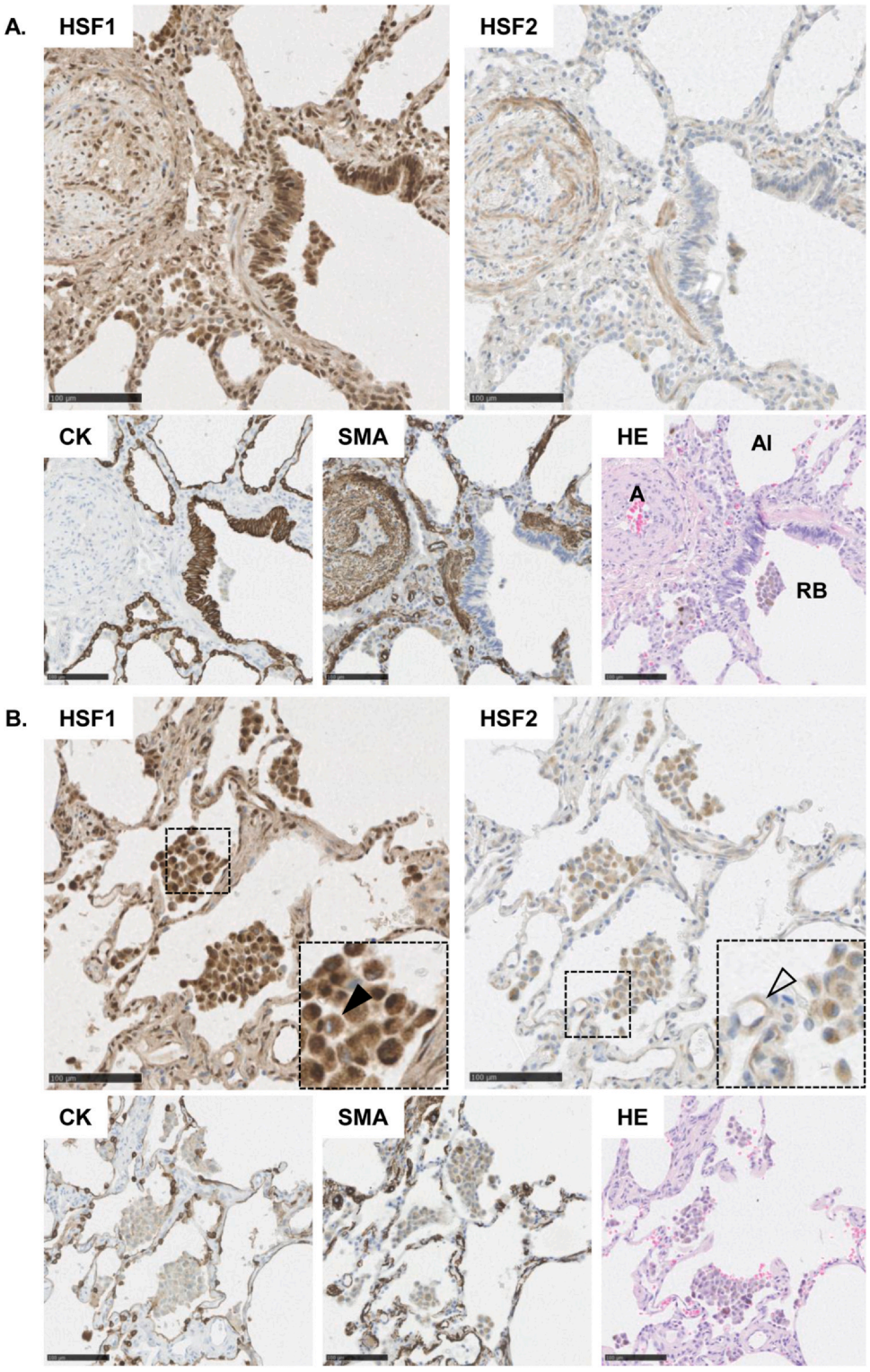

Fig. 10 Cross-section of the lung. (A) HSF1 is expressed in the nucleus and cytoplasm of CK-positive respiratory epithelial cells and pneumocytes. HSF2 is undetectable in the respiratory epithelia but displays moderate expression in the SMA-positive smooth muscle cells of respiratory bronchioles and arteries. Scale bar 100 μm. (B) Alveolar macrophages. HSF1 displays strong expression in alveolar macrophages, where it localizes in the nucleus and cytoplasm of most but not all cells. Moderate expression of HSF2 is detected in the alveolar macrophages and the endothelial cells of pulmonary capillaries. In the HSF1 inset, the arrowhead indicates absence of nuclear HSF1 in individual alveolar macrophages. In the HSF2 inset, the open arrowhead indicates cytoplasmic expression of HSF2 in the pulmonary capillary endothelia. Scale bar 100 μm. Abbreviations used: A, pulmonary artery; Al, alveolus; CK, pan-cytokeratin; HE, hematoxylin and eosin; RB, respiratory bronchiole; SMA, alpha-smooth muscle actin.

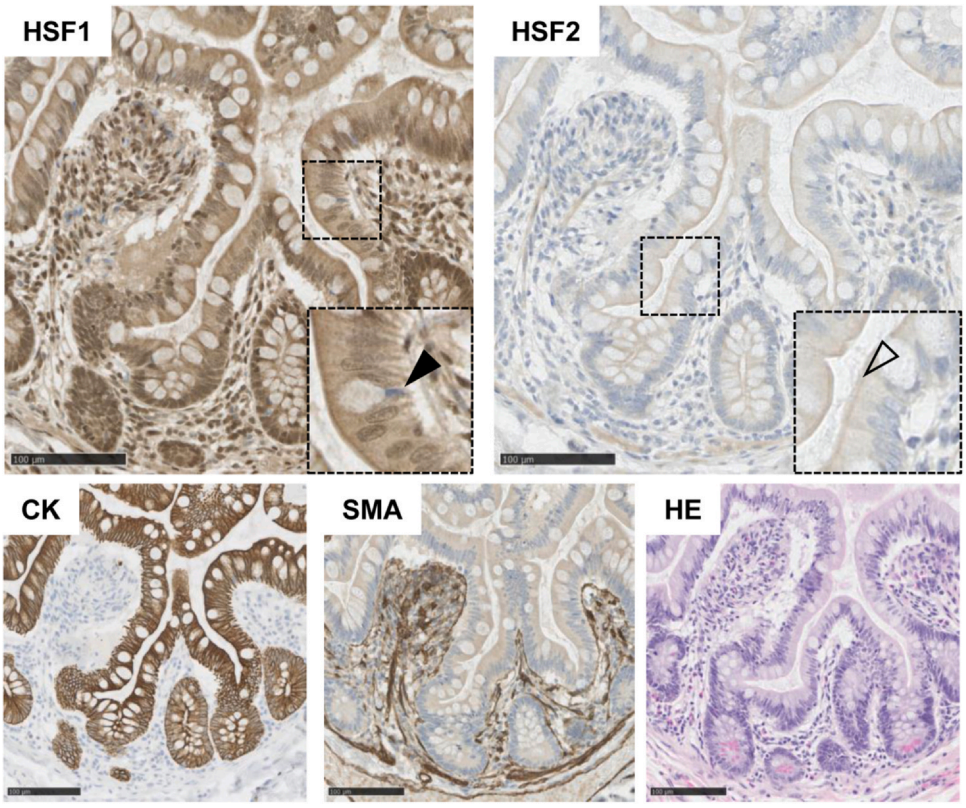

Fig. 11 Cross-section of the small intestine. HSF1 is strongly expressed in the nucleus and cytoplasm of the CK-positive enterocytes but localizes only to the cytoplasm of Goblet cells. HSF2 displays moderate cytoplasmic expression pattern in the enterocytes with a putative concentration at the apical junctional complex underlining the microvilli. In the HSF1 inset, the arrowhead indicates absence of nuclear expression of HSF1 in a Goblet cell. In the HSF2 inset, the open arrowhead indicates concentration of HSF2 at the apical adhesion belt. Scale bar 100 μm. Abbreviations used: CK, pan-cytokeratin; HE, hematoxylin and eosin; SMA, alpha-smooth muscle actin.

intestinal and colonic samples, the rectal Goblet cells lacked nuclear HSF1 expression (Figure 13).

Pancreas

The pancreas is an elongated glandular organ that regulates both the digestive and endocrine systems of the human body. The majority of the pancreatic tissue has an exocrine role and organizes as small acini secreting digestive enzymes into the intercalated pancreatic ducts. The acinar cells are pyramid-shaped cells with large cytoplasmic granules and a nucleus localized close to the basement membrane. HSF1 was moderately expressed in the nucleus and cytoplasm of the acinar cells, while no signal of HSF2 could be observed in these cells (Figure 14(A)). The intercalated ducts drain into intralobular ducts, which ultimately converge to the main pancreatic duct. The pancreatic ductal network is composed of simple columnar epithelium with a thin layer of surrounding connective tissue. Similarly to other epithelial cell types, HSF1 was strongly expressed in the nucleus and cytoplasm of the ductal cells (Figure 14(A)). Interestingly, weak cytoplasmic expression of HSF2 was also observed in the intralobular pancreatic duct epithelia (Figure 14(A)).

The endocrine pancreas is organized as separate pancreatic islets, also called the islets of Langerhans, that are surrounded by the exocrine acini. Pancreatic islets contain a variety of different cell types, including the α-cells secreting glucagon, β-cells secreting insulin, and the endothelial cells forming the small arterioles that allow hormone entry into the systemic circulation. Strikingly, both HSF1 and HSF2 displayed strong signals in distinct endocrine islet cells, with HSF1 localizing in the nucleus and cytoplasm, and HSF2 exclusively in the cytoplasm (Figure 14(B)). As the used tissue markers (CK and SMA) are not sufficient to identify distinct cell phenotypes, one can only speculate on the cell-type specificity of HSF expression. Previous investigations of the islet architecture have revealed that in the human pancreas, β-cells often localize as lobules that are surrounded by a mantle of α-cells and other endocrine cell types.[31] Considering the cytoplasmic expression of HSF2 in the outermost islet cells (Figure 14(B)), it is possible that HSF2 resides specifically in the α-cells. However, further studies should conclusively determine the cell-type-

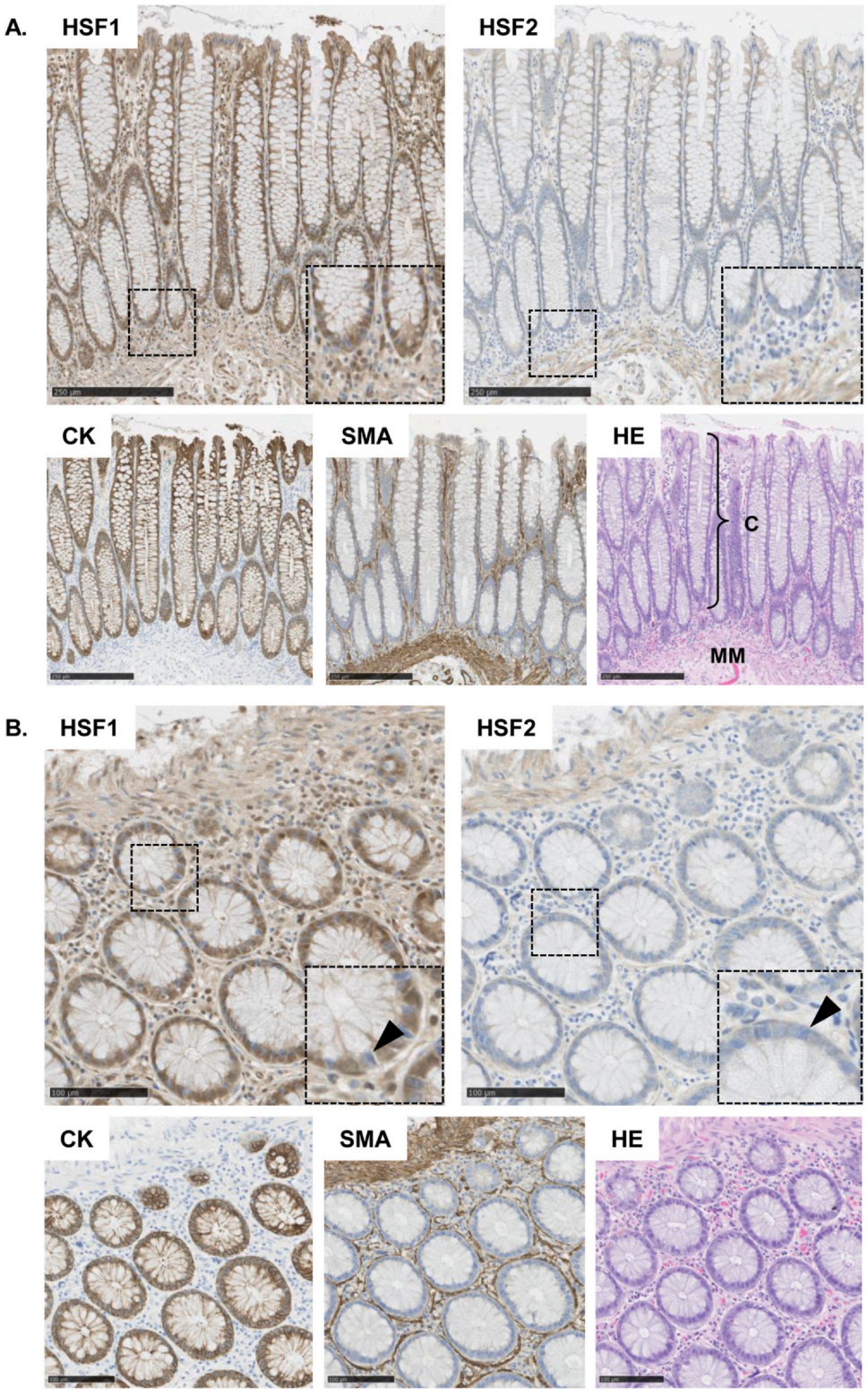

Fig. 12 Cross-section of the colon. HSF1 is present in the nucleus and cytoplasm of the colonic enterocytes, but localizes only to the cytoplasm of the Goblet cells. Weak expression of HSF2 is detected in the cytoplasm of the enterocytes and in the SMA-positive smooth muscle cells forming the intestinal muscularis mucosa. (A) Longitudinal section. The HSF1 and HSF2 insets highlight the stem cell compartment of colonic crypts harboring the stem cells and Paneth cells. Scale bar 250 μm. (B) Transverse section. In the HSF1 and HSF2 insets, the arrowheads indicate absence of nuclear expression of HSF1 and HSF2 in Goblet cells. Scale bar 100 μm. Abbreviations used: C, colonic crypt; CK, pan-cytokeratin; HE, hematoxylin and eosin; MM, muscularis mucosae; SMA, alpha-smooth muscle actin.

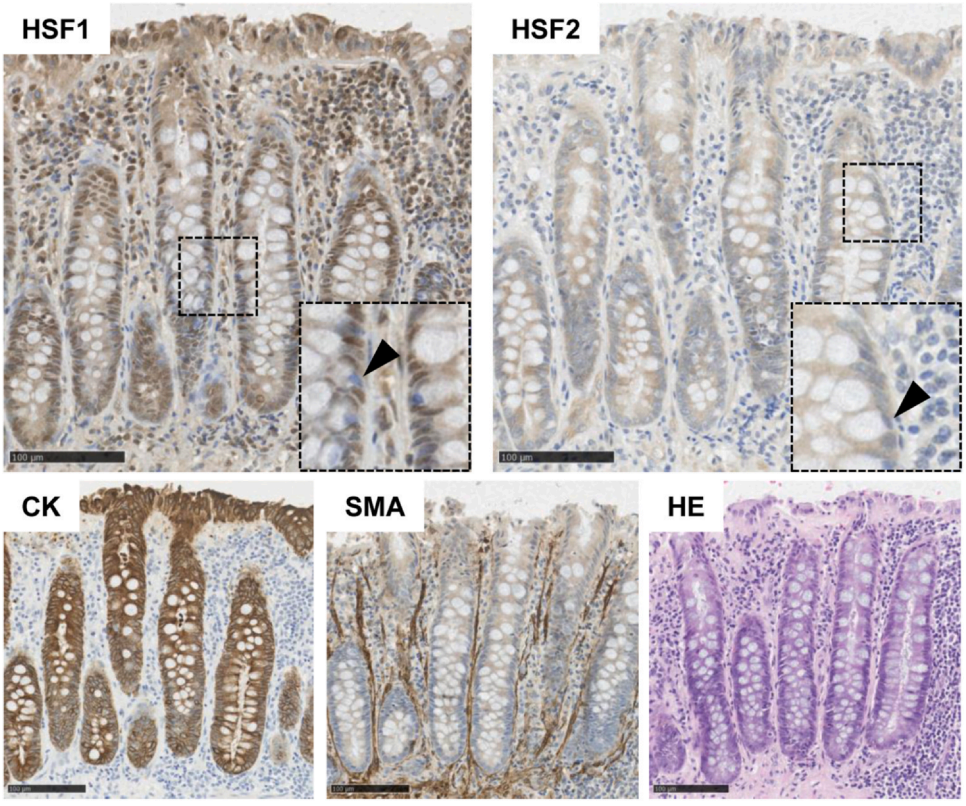

Fig. 13 Cross-section of the rectum. The rectal enterocytes show strong expression of HSF1 in the nucleus and cytoplasm, whereas only moderate expression of HSF2 is observed in the cytoplasm. In the HSF1 and HSF2 insets, the arrowheads indicate absence of nuclear expression of HSF1 and HSF2 in Goblet cells. Scale bar 100 μm. Abbreviations used: CK, pan-cytokeratin; HE, hematoxylin and eosin; SMA, alpha-smooth muscle actin.

specific expression patterns of HSF1 and HSF2 in the endocrine pancreas.

Liver

The liver is the largest internal organ, and it has a plethora of functions relevant to organismal homeostasis, including detoxification of metabolic waste products, synthesis of plasma proteins, and secretion of bile acids. The organ is structured by hexagonal hepatic lobules that harbor hepatocytes and sinusoids radiating from the central vein toward the periphery of the lobule. The polyhedral hepatocytes are responsible for nearly all functions of the liver, whereas the sinusoids carry blood from the hepatic artery and portal vein to the central vein. The sinusoids are lined by hepatic sinusoidal endothelial cells and accommodate the liver macrophages, the Kupffer cells. Interestingly, we found that HSF1 is undetectable in the nuclei of benign hepatocytes but shows a strong nuclear signal in the sinusoidal phagocytic Kupffer cells (Figure 15(A)). These findings are in line with the HPA and with recent findings, demonstrating nuclear expression of HSF1 only in cirrhotic hepatocytes.[32] The adult hepatocytes have three distinct membrane domains, i.e., sinusoidal, lateral, and canalicular, of which the canalicular membrane domain is responsible for forming the bile canalicular network that transports bile to the portal triad and to the intrahepatic bile ducts. The canaliculi are surrounded by lateral membrane domains that serve as active sites of cell–cell adhesion and are thus essential for the formation of the blood-bile barrier.[33] Albeit HSF2 was undetectable in the nucleus or cytoplasm of the hepatocytes or the sinusoidal cells, HSF2 was clearly localized in the canaliculi (Figure 15(A)). These results provide yet another example of HSF2 localizing at cell–cell adhesion contacts.

Portal triads reside at the junctions of hepatic lobules and consist of portal veins, hepatic arteries, bile ducts, and lymphatic vessels. Portal veins are large in diameter and carry nutrient-enriched and toxin-enriched blood from the gastrointestinal tract to the liver sinusoids. The bile in the interlobular bile ducts flows in the opposite direction and empties into the common hepatic bile duct. Intrahepatic bile ducts are lined by cuboidal epithelial cells, so-called cholangiocytes, that modify the hepatocyte-derived bile. In agreement with other samples containing vasculature, we observed a strong

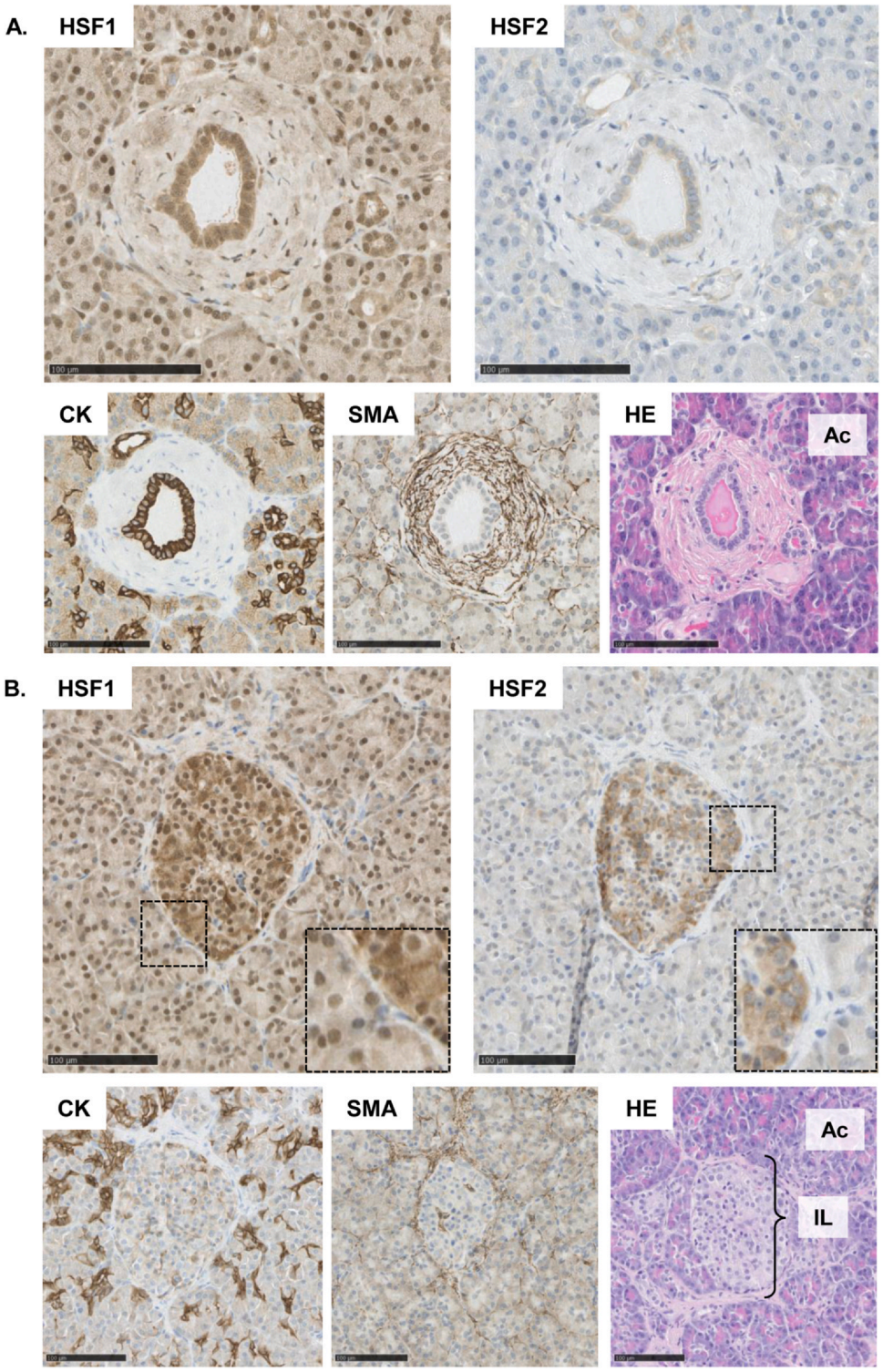

Fig. 14 Cross-section of the pancreas. (A) Intralobular pancreatic duct surrounded by acinar cells. HSF1 is strongly expressed in the nucleus and cytoplasm of the ductal cells, but HSF2 expression is weak. In the acinar cells, HSF1 expression is moderate in the nucleus and cytoplasm, while no signal of HSF2 is observed. (B) Islet of Langerhans. Both HSF1 and HSF2 display strong signal in distinct endocrine islet cells, with HSF1 localizing in the nucleus and cytoplasm, and HSF2 exclusively in the cytoplasm. Scale bar 100 μm. Abbreviations used: Ac, acinar cells; CK, pan-cytokeratin; HE, hematoxylin and eosin; IL, Islet of Langerhans; SMA, alpha-smooth muscle actin.

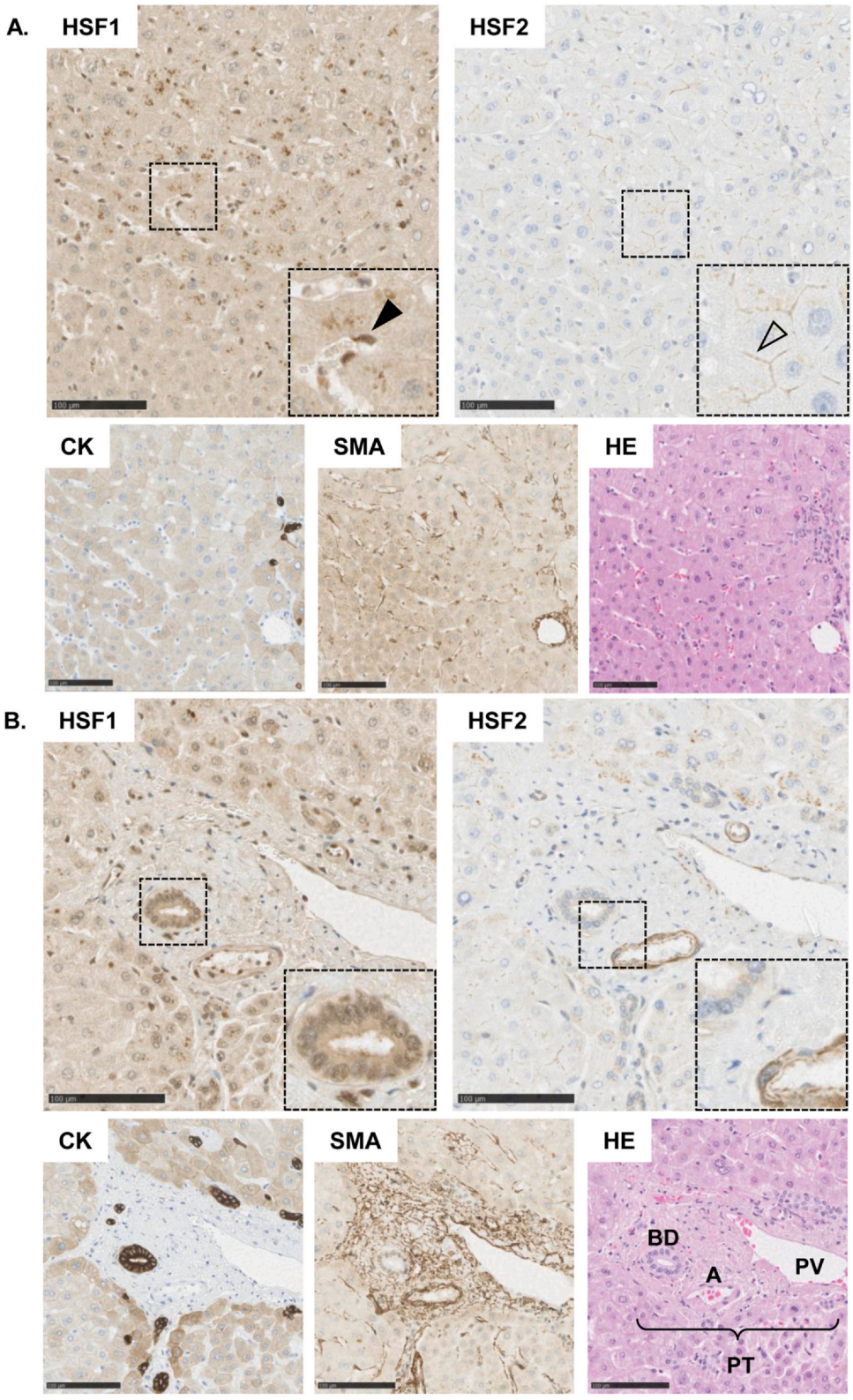

Fig. 15 Cross-section of the liver. (A) The hepatocytes and sinusoids. HSF1 is undetectable in the nuclei of hepatocytes but shows nuclear signal in the Kupffer cells. No signal of HSF2 is observed in the nucleus or cytoplasm of hepatocytes. HSF2 localizes to bile canaliculi. In the HSF1 inset, the arrowhead indicates HSF1 localization to sinusoidal Kupffer cells. In the HSF2 inset, the open arrowhead indicates HSF2 localization to bile canaliculus. (B) Portal triad. Expression of HSF1 is observed in the nucleus and cytoplasm of endothelial and smooth muscle cells and in the CK-positive cholangiocytes. HSF2 is expressed only in the cytoplasm of endothelial and smooth muscle cells. Scale bar 100 μm. Abbreviations used: A, artery; BD, bile duct; CK, pan-cytokeratin; HE, hematoxylin and eosin; PT, Portal triad; PV, portal vein; SMA, alpha-smooth muscle actin.

expression of HSF1 in the nucleus and a moderate expression of HSF2 in the cytoplasm of endothelial and smooth muscle cells of portal veins and arteries (Figure 15(B)). In the CK-positive cholangiocytes, HSF1 localized to both the nucleus and cytoplasm (Figure 15(B)), while no signal of HSF2 was observed in these cells (Figure 15(B)).

Urinary system

The urinary system regulates water and electrolyte balance, and it consists of kidneys, ureters, urinary bladder, and urethra. The basic structural and functional unit of the kidney is called a nephron and is composed of a renal corpuscle and a long convoluted renal tubule. Renal tubules are further divided into sections of the proximal convoluted tubule, loop of Henle, and a distal convoluted tubule. Nephrons localize both in the outer cortex and in the inner medulla of the kidney, but the renal corpuscles harboring the glomeruli, Bowman´s capsule, and the juxtaglomerular apparatus are only present in the cortex. By investigating cross-sections of the renal cortex, we found that HSF1 localizes in the nucleus and cytoplasm of all epithelial cells of the renal tubule. However, the expression level varied between the tubular sections, with cells of distal convoluted tubules generating the strongest and the cells of proximal convoluted tubules the weakest HSF1 signal (Figure 16(A)). Although the expression of HSF2 varied between the tubular sections, the localization was constantly restricted to the cytoplasm (Figure 16(A)). The renal glomerulus is structured by endothelial cells that form the glomerular capillaries and podocytes that contribute to renal filtration. The capillary structures are supported by stalks of connective tissue with macrophage-like mesangial cells. In the glomerulus, the expression and subcellular localization of HSF1 and HSF2 were markedly heterotypic (Figure 16(A)), indicating that HSFs are expressed in a cell-type-dependent manner in the human glomerulus. The renal medulla is arranged into medullary rays that consist of the straight portion of the proximal convoluted tubules, the ascending limb of Henle, and the straight collecting tubules. In the renal medulla, we observed weak HSF1 expression in the nucleus and cytoplasm of all tubular epithelial cells (Figure 16(B)), whereas HSF2 was undetectable in the medullary tubules (Figure 16(B)).

The ureters are muscular tubes leading from the renal pelvis to the urinary bladder. The mucosal surfaces of the ureters and the urinary bladder are covered by transitional epithelium, which is a highly specialized stratified epithelium capable of changing its shape and structure in response to stretching. The main function of the transitional epithelium is to act as a barrier between the lumen of the urinary tract and the bloodstream, and thus protect against environmental stressors, including osmotic stress, toxic substances, and pathogens.[34] The transitional epithelium divides into three layers of cells: the superficial cells, intermediate cells, and basal cells. The renewal of the epithelium is covered by the progenitor-like basal cells and highly proliferative intermediate cells.[34] The superficial cells, also called umbrella cells, are fully differentiated and responsible for the barrier function. To achieve this, the umbrella cells are tightly connected by virtually impenetrable cell–cell adhesion contacts that seal the cells together. In our samples of the ureters and urinary bladders, we observed a strong expression of HSF1 in the nucleus and cytoplasm of cells in all layers of the transitional epithelium (Figure 17(A) and (B)). In contrast, HSF2 was only moderately expressed in the cytoplasm of the intermediate and basal cells but strikingly displayed a robust nuclear expression in the luminal umbrella cells (Figure 17(A) and (B)). Due to the notable expression of HSF2 in the nucleus of umbrella cells, we investigated the expression pattern of HSF2 also in the urinary bladder samples of HPA. Intriguingly, distinct nuclear localization of HSF2 was observed also in the samples of HPA (Urinary bladder, ID1870), suggesting that HSF2 might be activated specifically in the umbrella cells of the transitional epithelium.

Testes

The testes are paired organs responsible for the production of sperm and androgens. The parenchyma of the testis is composed of seminiferous tubules producing sperm and interstitial connective tissue containing blood vessels and the Leydig cells. The seminiferous tubules are lined by stratified germinal epithelium with two main cell populations: the spermatogenic cells and the supporting cells. The spermatogenic cells, namely spermatogonia, spermatocytes, round spermatids, and spermatozoa, are arranged in layers that sequentially differentiate from the basal layers toward the lumen of the tubule. Testis is one of the few mammalian tissue types where the expression, localization, and functional relevance of HSF1 and HSF2 have been previously characterized.[35] In adult rodent seminiferous tubules, Hsf2 was reported to be most abundant in the pachytene spermatocytes and round spermatids.[17,36] In accordance with the expression pattern, Hsf2-null mice display multiple testicular defects, including reduced testis size, abnormal tubule morphology, and reduced amount of

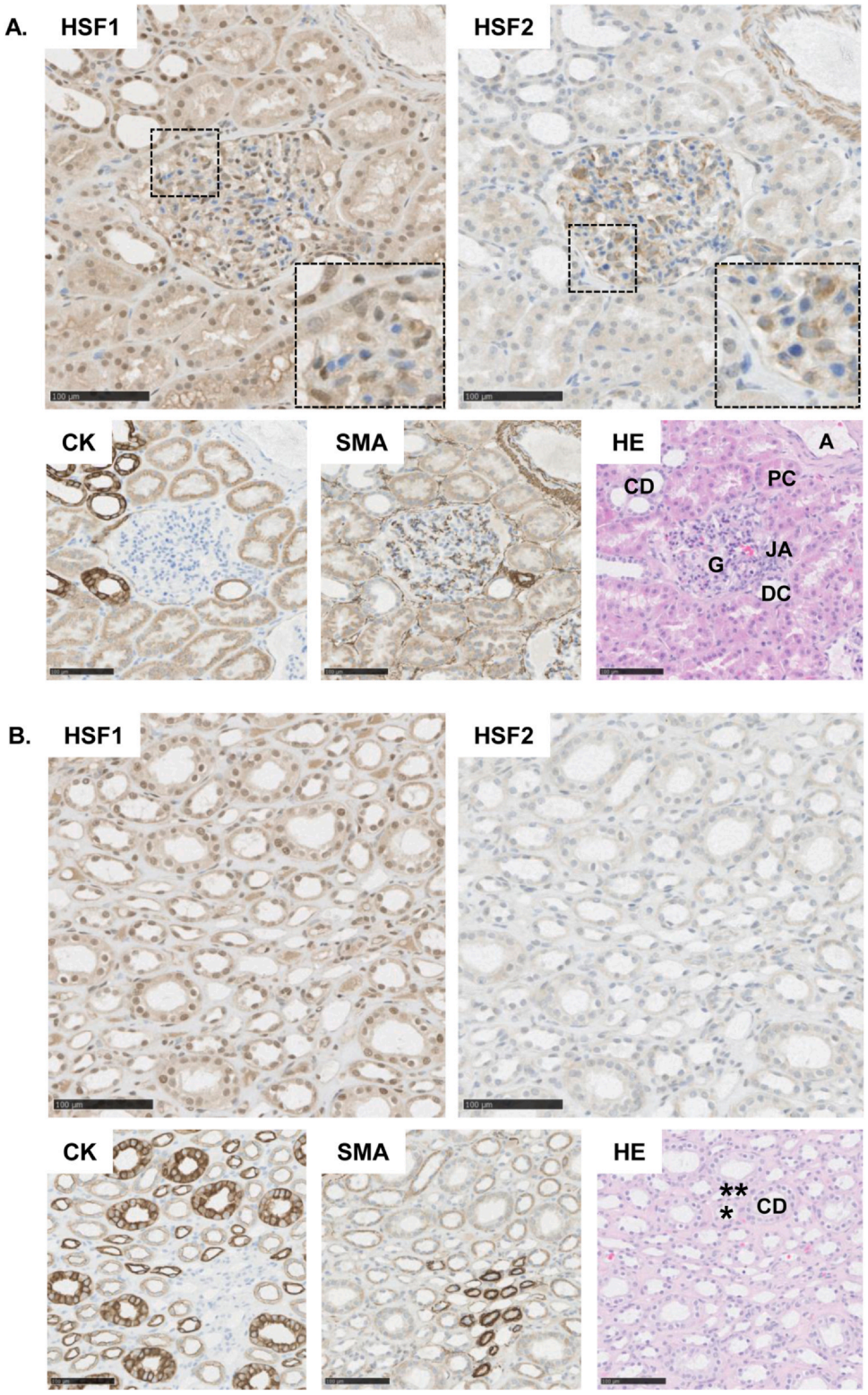

Fig. 16 Cross-section of the kidney. (A) Renal cortex. HSF1 localizes in the nucleus and cytoplasm of all epithelial cells of the cortical tubules. HSF2 localization is cytoplasmic. Both HSF1 and HSF2 display heterotypic expression pattern in the cells of renal glomeruli. The HSF1 inset highlights the nuclear expression of HSF1 in only distinct glomerular cells. The HSF2 inset highlights the cytoplasmic expression of HSF2 in only distinct glomerular cells. Scale bar 100 μm. (B) Renal medulla. HSF1 localizes in the nucleus and cytoplasm of the epithelial cells of the medullary tubules, while HSF2 is undetectable. Scale bar 100 μm. The double asterisk denotes the thin descending limb of loop of Henle; the asterisk denotes the thick ascending limb of loop of Henle. Abbreviations used: A, artery; CD, collecting duct; CK, pan-cytokeratin; DC, distal convoluted tubule; G, glomerulus; HE, hematoxylin and eosin; JA, juxtaglomerular apparatus; PC, proximal convoluted tubule; SMA, alpha-smooth muscle actin.

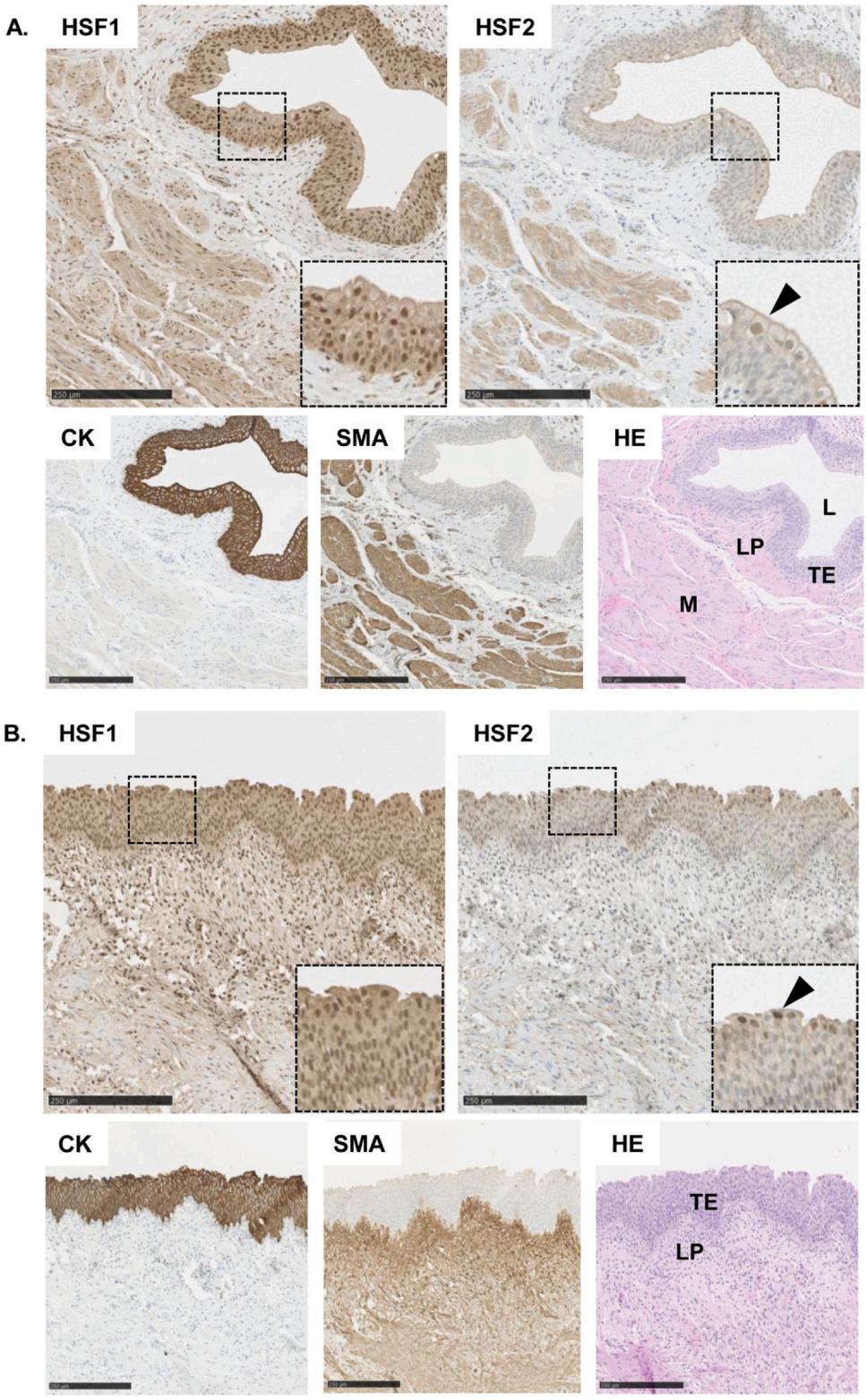

Fig. 17 Cross-sections of the urethra and the bladder. HSF1 is expressed in the nucleus and cytoplasm of cells in all layers of the transitional epithelium. HSF2 is moderately expressed in the cytoplasm of the intermediate and basal cells but displays nuclear expression in the superficial umbrella cells. (A) Transitional epithelium of the urethra. In the HSF2 inset, the arrowhead indicates HSF2 localization to superficial umbrella cells. Scale bar 250 μm. (B) Transitional epithelium of the bladder. In the HSF2 inset, the arrowhead indicates HSF2 localization to superficial umbrella cells. Scale bar 250 μm. Abbreviations used: CK, pan-cytokeratin; HE, hematoxylin and eosin; L, lumen; LP, lamina propria; M, muscularis; SMA, alpha-smooth muscle actin; TE, transitional epithelium.

spermatozoa.[22,23] Although the lack of Hsf1 alone does not cause marked defects in mice spermatogenesis,[37] disruption of both Hsf1 and Hsf2 genes leads to complete male sterility.[26] Interaction of Hsf1 and Hsf2 in mouse testes occurs through heterotrimerization[38] and contributes to the maintenance of proper chromatin organization[24] and transcriptional regulation of distinct target genes.[39] By investigating the cross-sections of human testes samples, we found that both HSF1 and HSF2 are strongly expressed in the nucleus of basal spermatogonia stem cells (Figure 18). Also, other spermatogenic cell types harbored nuclear HSF1 and HSF2, but to a lesser extent (Figure 18). Neither HSF1 nor HSF2 was observed in the mature spermatozoa (Figure 18). Albeit these findings slightly differ from those of rodent tissues, our results are well in line with HSF1 and HSF2 stainings of human testes samples presented in the HPA (e.g., HSF1: ID2071 and HSF2: ID2435).

Epididymis and vas deferens

The matured spermatozoa travel from the convoluted seminiferous tubules *via* the rete testis to the epididymis, which functions as a storage site for sperm. The convoluted epididymal duct is lined by pseudostratified epithelium composed of tall columnar cells and basal cells. The columnar cells function in the resorption of fluid and have nonmotile stereocilia at their apical surface. The functional relevance of the basal cells has remained unknown. Similarly to other epithelial cell types, HSF1 was strongly expressed in the nucleus and cytoplasm of both columnar and basal cells (Figure 19(A)). Intriguingly, HSF2 localized predominantly at the membranes of the columnar cells with a distinct accumulation at the apical cell–cell adhesion contacts (Figure 19(A)). Due to the pyramidal shape and small amount of cytoplasm in basal cells, we were unable to conclusively define whether HSF2 localizes at the membrane or the cytoplasm of the basal cells (Figure 19(A)).

Mature sperm exits the epididymis through the vas deferens, which is a fibromuscular tube connecting the epididymal duct to the urethra. The mucosa of vas deferens is a pseudostratified columnar epithelium that folds longitudinally allowing the rapid expansion of the duct during ejaculation. A thick muscular layer surrounds the duct, which enables the rapid contraction of the organ. As in the epithelia lining of the epididymal duct (Figure 19(A)), HSF1 was strongly expressed in the nucleus and cytoplasm of the CK-positive epithelial cells of vas deferens (Figure 19(B)). HSF2 was localized at the plasma membrane of both columnar and basal cells (Figure 19(B)). Similarly to the smooth muscle cells surrounding the vasculature (Figure 6(A)), abundant cytoplasmic HSF2 was also found in the smooth muscle cells forming the thick muscularis of vas deferens (Figure 19(B)).

Mammary gland

The tubuloacinar mammary glands form the major component of the female breasts. Mammary glands are composed of a variable number of lobes that further divide into lobules containing the terminal ductules and the intralobular ducts. The ductal system is lined by cuboidal epithelium, which at the level of interlobular ducts acquires a stratified, often double-layered, structure. A discontinuous layer of myoepithelial cells surrounds the epithelium, which, together with the basement membrane, provides structural support. By investigating the cross-sections of human breast tissue, we found that HSF1 is strongly expressed in the nucleus and cytoplasm of ductal epithelial cells (Figure 20(A)). In line with our findings from the sweat glands, HSF2 was observed in the cytoplasm of the SMA-positive myoepithelial cells surrounding the ductal epithelium (Figure 20(A)). In the resting mammary gland, the lobules appear as islands of glandular tissue without clear secretory acini. Similarly to the interlobular ducts, strong expression of HSF1 was found in the nucleus and cytoplasm of the lobular epithelial cells and HSF2 in the cytoplasm of the myoepithelial cells (Figure 20(B)). Previous work has demonstrated only a minute expression of HSF1 in normal breast epithelium,[28] but our findings are in line with HSF1 stainings presented in the HPA (ID2773). It is plausible that the variability of the observations is due to differences in the used antibodies in these studies.

Uterus and fallopian tubes

The wall of the human uterus consists of three functional layers: endometrium, myometrium, and perimetrium. In response to ovarian hormones, the endometrium undergoes a sequence of histological and physiological changes highlighted by the proliferative, secretory, and menstrual phases. The endometrium is composed of epithelium, uterine glands, and endometrial stroma, which all cooperate in the physiological alterations of uterine functions. The superficial epithelium is a simple columnar epithelium with a mixture of secretory and ciliated cells. The uterine glands extend through the full thickness of the endometrium and are lined by columnar epithelium with less ciliated cells. In our endometrial samples, HSF1 localized in the nucleus of the epithelial cells (Figure 21(A)). In some samples, also the cytoplasm of the epithelial cells stained strongly with HSF1. Weak expression of HSF2

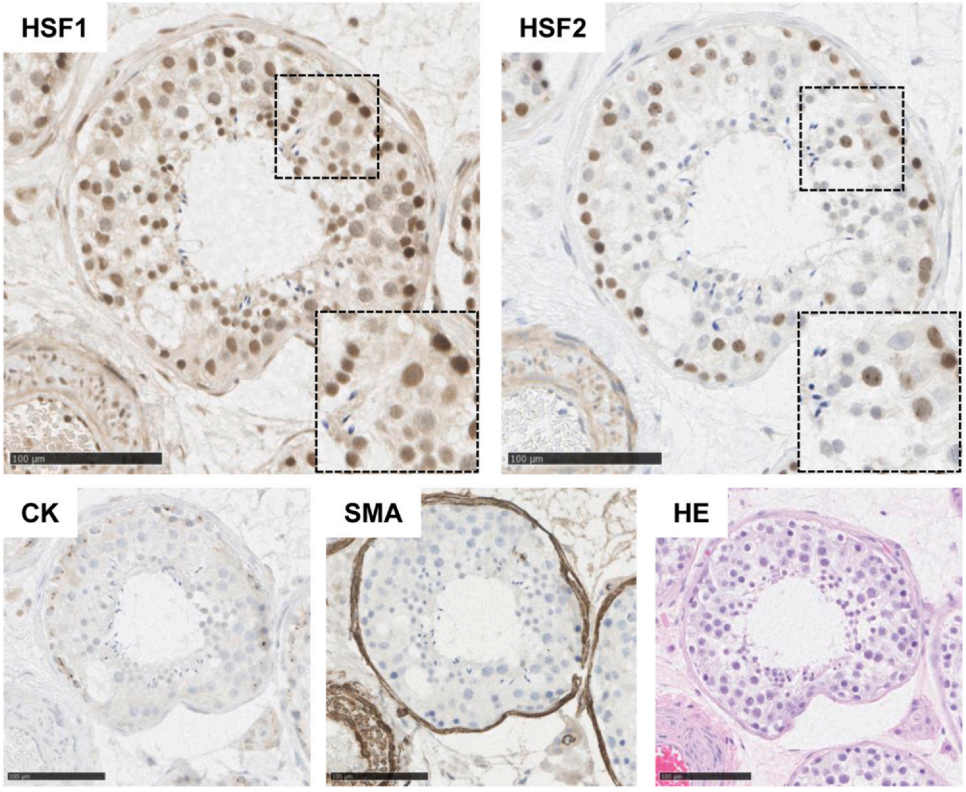

Fig. 18 Cross-section of testis. HSF1 and HSF2 are strongly expressed in the nucleus of basal spermatogonia stem cells. Neither HSF1 nor HSF2 is observed in the mature spermatozoa. The HSF1 and HSF2 insets highlight the nuclear expression of HSF1 and HSF2 in distinct cell types and full absence of HSF1 and HSF2 in the mature spermatocytes. Scale bar 100 μm. Abbreviations used: CK, pan-cytokeratin; HE, hematoxylin and eosin; SMA, alpha-smooth muscle actin.

was observed specifically in the epithelial cytoplasm. The endometrial stroma is a vascularized connective tissue with specific endometrial stromal cells, spiral arteries, and endometrial venules. During the secretory phase of the menstrual cycle, the stromal cells undergo morphological and functional changes and transform into decidual cells, ensuring embryo implantation. Interestingly, we observed strong expression of HSF1 only in the nucleus, while no signal of HSF2 was detected in the endometrial stromal cells (Figure 21(A)). In the myometrium, the smooth muscle cells are arranged as cylindrical bundles that interlace in all directions. During pregnancy, the myometrium increases in size in response to estrogen stimuli. In line with our findings from other smooth muscle tissues (Figures 6 and 19), HSF1 was prominently expressed in the nucleus and cytoplasm of the uterine myometrial cells, but HSF2 localized in the cytoplasm of the SMA-positive uterine smooth muscle cells (Figure 21(B)).

The fallopian tubes, or oviducts, are paired tubular organs that convoy the ova from the ovarian surface to the uterine cavity. The mucosa of the fallopian tubes is covered by simple columnar epithelium that consists of ciliated and nonciliated cells resting on a thin basement membrane. The function of the nonciliated cells is to produce a nutritious secretion that protects the transporting ovum. Ciliated cells are scattered between the nonciliated cells and bear numerous cilia beating toward the uterus. In our oviductal samples, HSF1 localized in the nucleus and cytoplasm of epithelial cells (Figure 22). Intriguingly, HSF2 localized in the nucleus of ciliated cells, displaying a clear cell-type specificity (Figure 22), which is in line with HSF2 stainings of fallopian tubes presented in the HPA (ID2447).

Discussion

The HSF-driven heat shock response is an evolutionarily conserved stress-protective mechanism that is characterized by extensive transcriptional reprogramming and upregulation of molecular chaperones.[1] The ability to survive protein-damaging stress is crucial for cell survival, and thereby it is not surprising that dysregulation of HSFs has been observed in a multitude of human pathologies. Recent genetic studies have provided invaluable resources for understanding the molecular details of stress-induced transcriptional reprogramming and for discovering new therapeutics targeting the heat shock response.[1,40,41] However, the current data originate predominantly from cancer cell

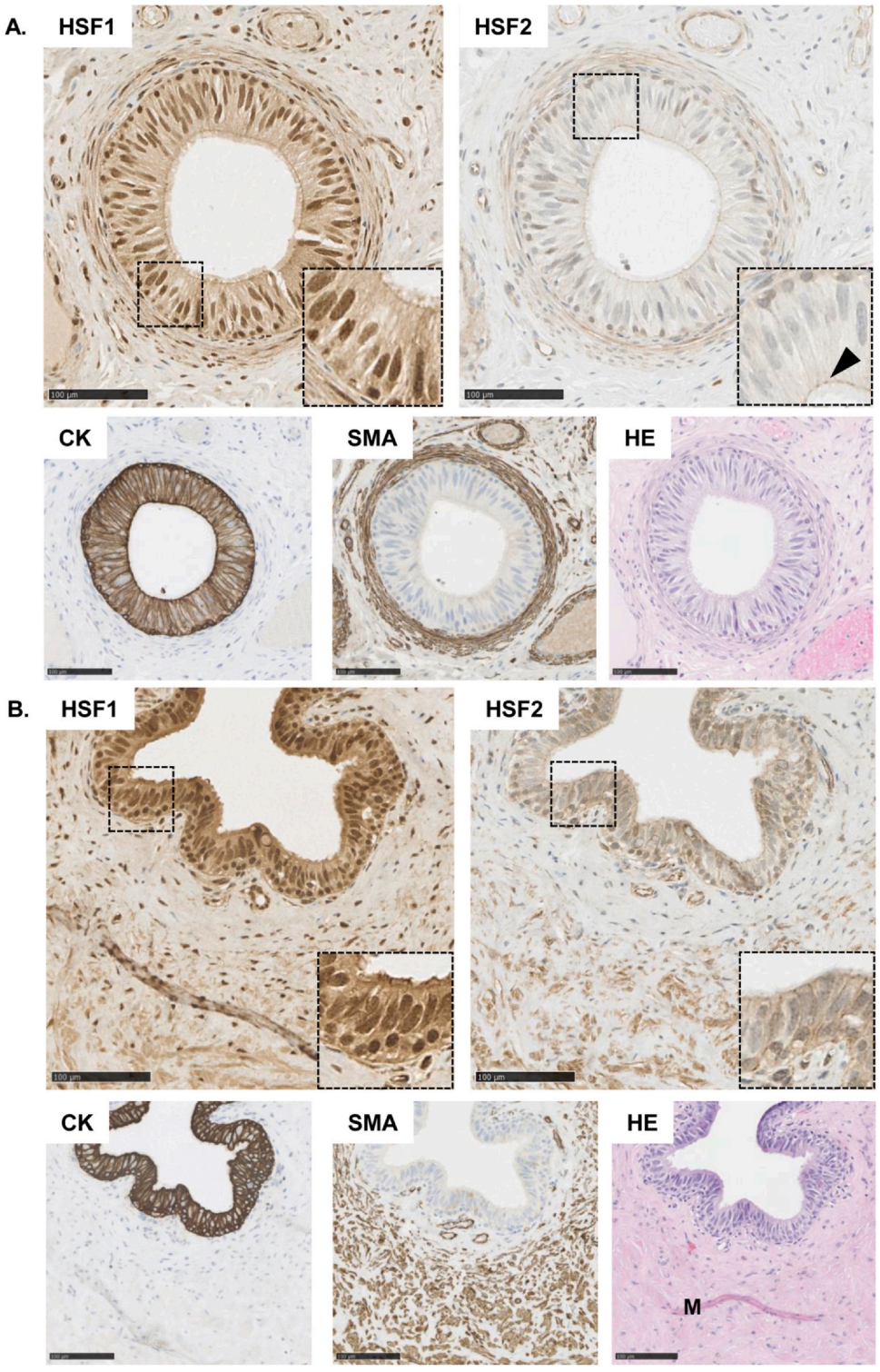

Fig. 19 Cross-section of (A) Caput of epididymis. HSF1 is strongly expressed in the nucleus and cytoplasm of both columnar and basal cells. HSF2 localizes predominantly at the membranes of the columnar cells and accumulates at the apical cell–cell adhesion contacts. The HSF1 inset highlights the nuclear and cytoplasmic expression of HSF1 in basal and columnar epithelial cells. In the HSF2 inset, the arrowhead indicates HSF2 localization to the apical plasma membrane of the epithelial cells. Scale bar 100 μm. (B) Vas deferens. HSF1 is strongly expressed in the nucleus and cytoplasm of CK-positive epithelial cells, while HSF2 localizes at the plasma membrane of both columnar and basal cells. Cytoplasmic HSF2 is detected in the smooth muscle cells. The HSF1 inset highlights the nuclear and cytoplasmic expression of HSF1 in the epithelial cells. The HSF2 inset highlights the localization of HSF2 to the plasma membrane of basal and columnar epithelial cells. Scale bar 100 μm. Abbreviations used: CK, pan-cytokeratin; HE, hematoxylin and eosin; M, smooth muscle layer; SMA, alpha-smooth muscle actin.

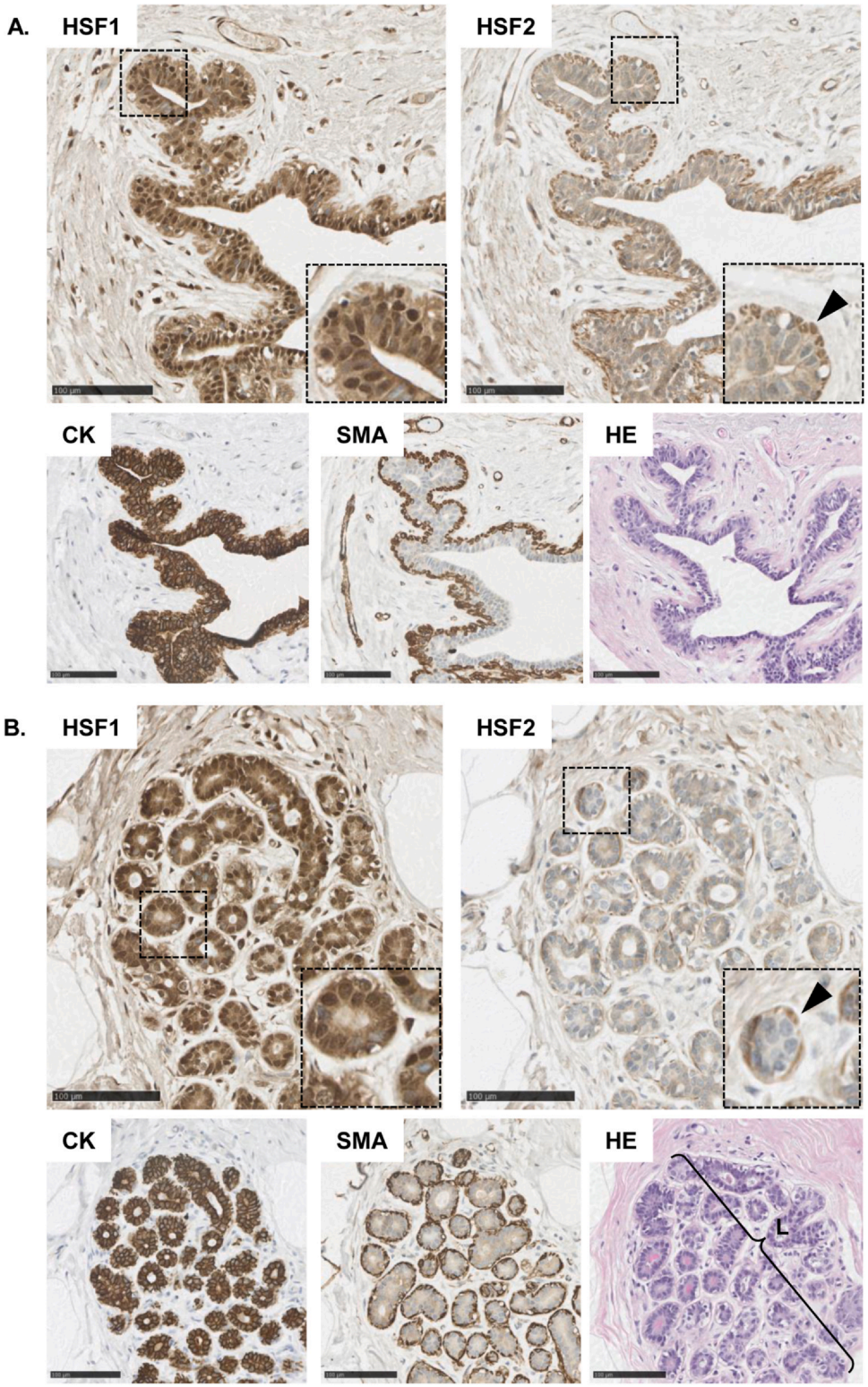

Fig. 20 Cross-section of the mammary gland. (A) Interlobular duct. HSF1 is strongly expressed in the nucleus and cytoplasm of ductal epithelial cells, while HSF2 localizes in the SMA-positive myoepithelial cells surrounding the ductal epithelium. The HSF1 inset highlights the nuclear and cytoplasmic expression of HSF1 in the epithelial cells. In the HSF2 inset, the arrowhead indicates cytoplasmic expression of HSF2 in the basal myoepithelial cells. Scale bar 100 μm. (B) Intralobular terminal ductules. HSF1 is strongly expressed in the nucleus and cytoplasm of lobular epithelial cells, while HSF2 localizes in the SMA-positive myoepithelial cells. The HSF1 inset highlights the nuclear and cytoplasmic expression of HSF1 in the epithelial cells. In the HSF2 inset, the arrowhead indicates cytoplasmic expression of HSF2 in the basal myoepithelial cells. Scale bar 100 μm. Abbreviations used: CK, pan-cytokeratin; HE, hematoxylin and eosin; L, breast lobule with terminal ductules; SMA, alpha-smooth muscle actin.

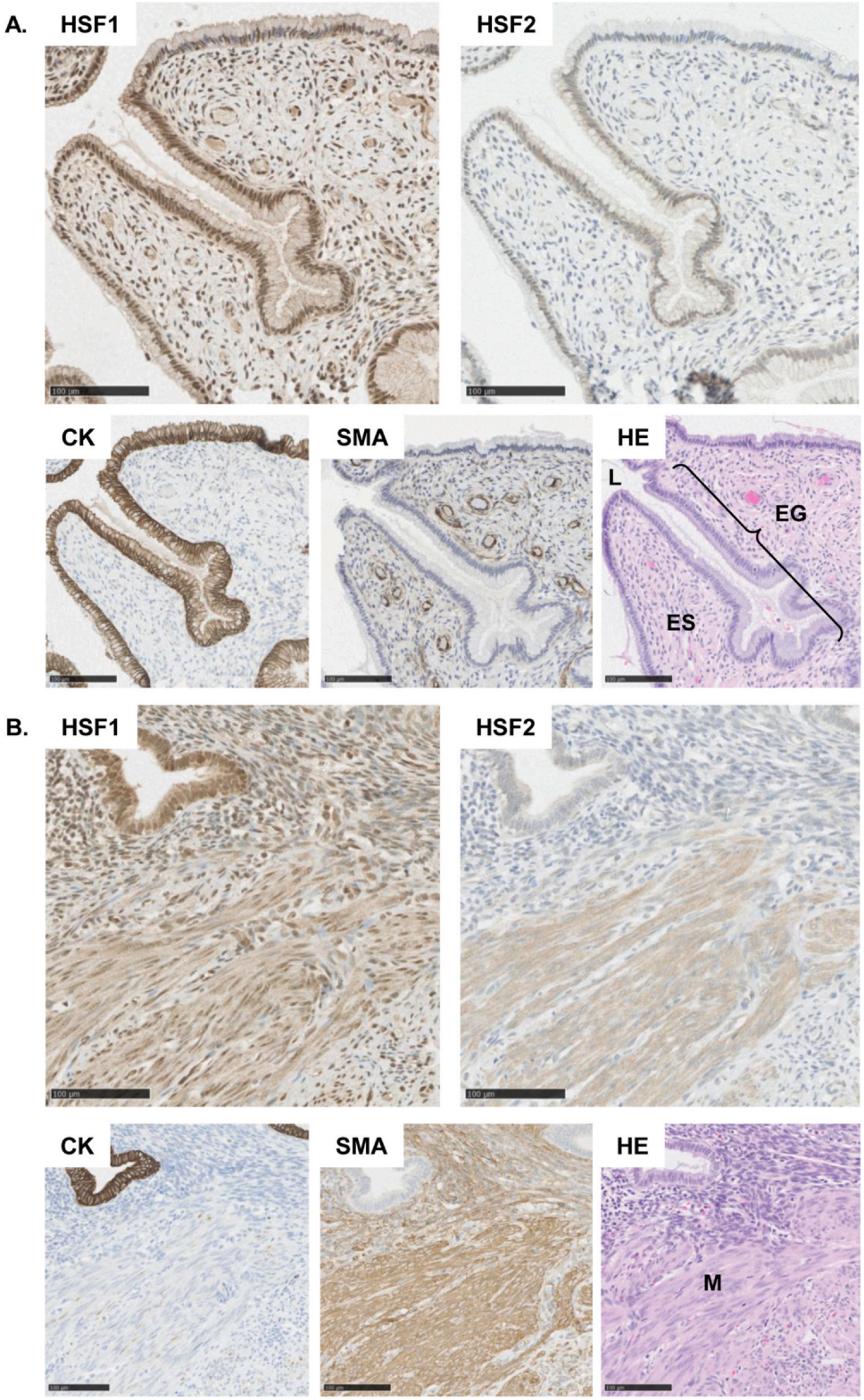

Fig. 21 Cross-section of the uterus (Stadium secretionis). (A) Endometrium. HSF1 localizes in the nucleus of endometrial epithelial cells, while HSF2 localizes in the cytoplasm. Strong expression of HSF1 is detected in the nucleus of endometrial stromal cells, while HSF2 is undetectable. (B) Myometrium. HSF1 is expressed in the nucleus and cytoplasm of the uterine myometrial cells, but HSF2 localizes in the cytoplasm of the SMA-positive uterine smooth muscle cells. Scale bar 100 μm. Abbreviations used: CK, pan-cytokeratin; EG, endometrial gland; ES, endometrial stroma; HE, hematoxylin and eosin; L, lumen; M, smooth muscle layer; SMA, alpha-smooth muscle actin.

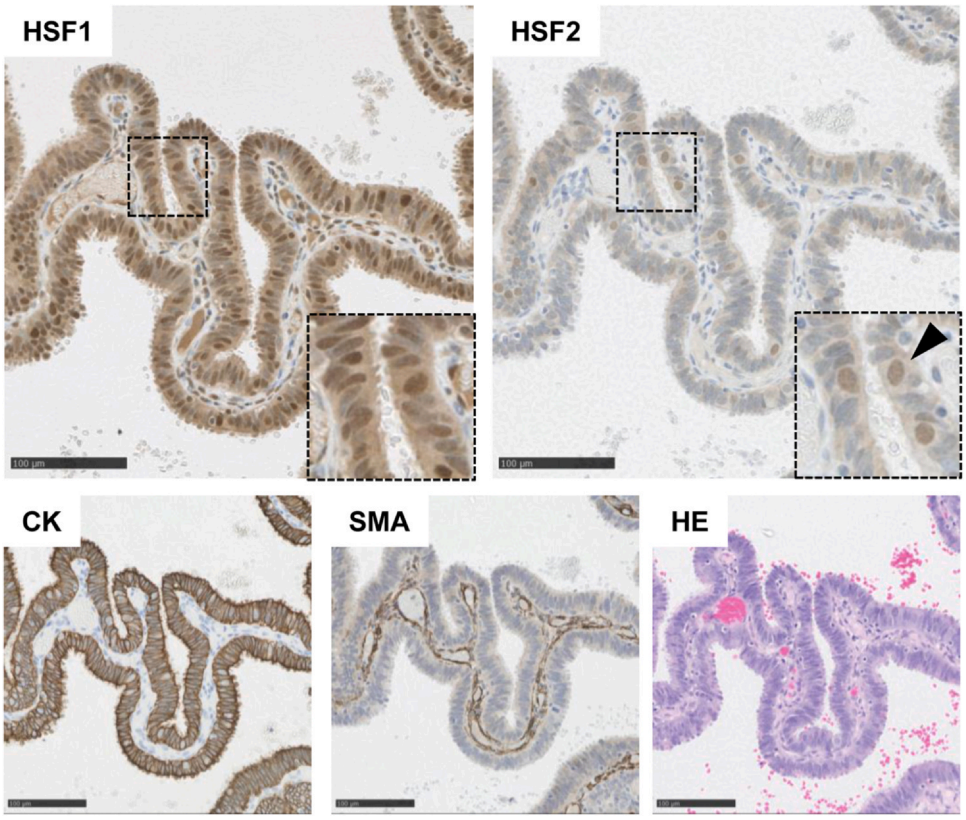

Fig. 22 Cross-section of a fallopian tube. HSF1 localizes in the nucleus and cytoplasm of epithelial cells, whereas HSF2 localizes in the nucleus of ciliated cells. The HSF1 inset highlights the nuclear localization of HSF1 in tubal epithelial cells. In the HSF2 inset, the arrowhead indicates nuclear localization of HSF2 in the ciliated cells of fallopian tubes. Scale bar 100 μm. Abbreviations used: CK, pan-cytokeratin; HE, hematoxylin and eosin; SMA, alpha-smooth muscle actin.

lines and tumor samples that are not adequate in portraying the importance of HSFs benign human tissues. To increase our understanding of the role of HSFs in human physiology and organismal homeostasis, we investigated the cell-type specific expression and localization patterns of HSFs in a comprehensive selection of human tissue samples with immunohistochemistry. Among the wealth of observations provided by our data, two particularly intriguing topics emerge: the clearly different subcellular localization patterns and the distinct cell-type specificity of HSF1 and HSF2 across many tissues. Both findings strongly propose that, despite their close proximity in the phylogenetic tree,[35] HSF1 and HSF2 are significantly different transcription factors with unique functions in human tissues.

Translating subcellular localizations of HSFs to functional implications

Acquisition of the trimeric DNA-binding competent state is a key feature of the activation-attenuation cycle of HSF-dependent transcription.[42] Early findings in human erythroleukemia K562 cells demonstrated that in nonstressed cells HSF1 resides in the cytoplasm as an inactive monomer, whereas HSF2 exists primarily as a dimer.[43,44] Exposure to stress induces trimerization, and both homotrimers of these factors as well as HSF1-HSF2 heterotrimers, have been described.[38] Here, we found that in the majority of cell types, HSF1 localizes in the cytoplasm and the nucleus (Table 1), suggesting that both inactive and active forms of HSF1 co-exist in benign cells. Nuclear localization of HSF1 was observed specifically in epithelial cell types, which reflects a constant activation of HSF1 under homeostatic conditions in cells of epithelial origin. HSF1 has been shown to be markedly dysregulated in a variety of different carcinomas,[45] i.e., cancers of epithelial origin, which might reflect the requirement of active HSF1 in supporting epithelial integrity. Indeed, a recent study in nontumorigenic mammary cell lines demonstrated that abnormally high expression of HSF1 pushes the cells toward the mesenchymal phenotype.[46] In stark contrast to HSF1, nuclear localization of HSF2 was observed only in a few distinct cell types, including the spermatocytes and spermatogonia (Figure 18) and the urothelial umbrella cells (Figure 17). To our great surprise, HSF2 displayed a cytoplasmic localization pattern in the majority of human cell types. Previous immunoelectron microscopy analyses of rat

testes have revealed HSF2 in the cytoplasm of zygotene spermatocytes.[36] Altogether, these findings propose that in cells expressing HSF2, this factor is maintained predominantly in its inactive dimeric state. The cytoplasmic HSF2 in multiple cell types could indicate that the regulation of HSF2 activity is very stringent in homeostatic tissues. An obvious question to be addressed is how this subcellular localization of HSFs is achieved. HSF1 monomers are restricted in the cytoplasm by a multichaperone complex composed of HSP40, HSP70, and HSP90,[2] but the molecular mechanisms maintaining the cytoplasmic population of HSF2 are unclear. HSF2 has been shown to interact with HSP90 in nonstressed cells,[47] but whether this interaction mediates cytoplasmic retention requires further investigation.

An outstanding finding is the distinct membrane localization of HSF2 in several cell types (Table 1). Prior to this work, Hsf2 has been detected at the membrane of cytoplasmic bridges connecting spermatocytes and spermatids in rat testes.[36] Eminently, we found that HSF2 localizes at variable cell–cell adhesion sites, including the intercalated discs connecting cardiomyocytes (Figure 5(B)), the bile canaliculi between hepatocytes (Figure 15(A)), and the apical junctional complex confirming epithelial integrity (Figure 19(A)). Albeit these adhesion sites serve clearly different functions in intact tissues, they are all featured by the same transmembrane proteins composing tight junctions, adherens junctions, desmosomes, and gap junctions.[33,48,49] The transmembrane adhesion proteins form, together with cytoskeletal linkers and signal-transduction molecules, a multiprotein complex that mediates cell-extrinsic signals to the nucleus. Signal transmission occurs through the translocation of proteins from the membrane compartment to the nucleus, where they act as transcriptional regulators.[50] We hypothesize that when localized at cell–cell adhesion sites, HSF2 monitors the integrity of cell adhesion contacts. Previously, we have found that in human osteosarcoma U2OS cells, silencing of HSF2 led to marked down-regulation of genes encoding cadherin superfamily proteins forming adherens junctions.[14] In line with these results, deregulation of the HSF2-dependent expression of N-cadherin was recently shown to underlie the characteristic neuroepithelial defects observed in Rubinstein-Taybi syndrome.[30] We envision that analogously to the accumulation of misfolded proteins that titrate the chaperones away from HSF1, enabling HSF1 target gene binding, disrupted cell adhesion protein complexes release HSF2 from its membrane compartment to enable nuclear accumulation and target gene activation. Considering that HSF2 occupancy has been detected at genes coding for cell adhesion proteins in K562 cells[51] and in mouse testis,[39] the disruption of the membrane complex could form a feedback loop promoting the re-establishment of cell adhesion. Since the membrane-associated protein complexes determine cell polarity, epithelial integrity, and mechanical force transmission,[48] it is plausible that when localized at cell–cell adhesion sites, HSF2 participates in the regulation of multicellular tissue homeostasis. Future studies should explore if the subcellular localization of HSF2 changes, for example, in response to epithelial stretching or mechanical challenging of cardiomyocytes. The relevance of HSF2 in cell–matrix adhesions should also be examined, e.g., in the context of alternating stiffness of the extracellular matrix. Identification of the protein-interaction partners of HSF2 at the membrane and in other subcellular locations is of key importance for characterizing the molecular determinants of our findings.

HSF2 as a cellular surveillance factor regulating cell phenotype

HSF2 has been shown to be expressed in a wide range of rodent tissues,[27] but to the best of our knowledge, the protein levels of HSF2 have not been systematically investigated in benign human tissues. Unlike HSF1, HSF2 is considered an unstable protein under normal growth conditions, and the expression of HSF2 is tightly regulated both at the mRNA and protein levels, *via* microRNAs and the ubiquitin-proteasome system.[30,43,52,53] Consequently, we were surprised to detect prominent cytoplasmic HSF2 expression in all studied smooth muscle cells, endothelial cells, and myoepithelial cells (Table 1). The significant difference in signal intensity compared to cell lines, which typically display nuclear HSF2 expression, shows that HSF2 is differently regulated in intact tissues. Based on the prominent cytoplasmic HSF2 signal, it is likely that HSF2 is stabilized through a higher synthesis rate or reduced degradation. Since ubiquitination of HSF2 occurs at the chromatin,[53] it is possible that HSF2 is rapidly degraded after achieving its trimeric DNA-binding competent state. Such a mechanism would support our hypothesis of HSF2 functioning as a cellular surveillance factor, as a high pool of cytoplasmic HSF2 could ensure a rapid and transient response to different intracellular and extracellular signals. This hypothesis raises a question about what HSF2 could be surveilling in cells.

Although smooth muscle cells, endothelial cells, and myoepithelial cells are all specialized cell types with distinct functions and characteristics, they share some common denominators. All three cell types are characterized by an elongated or spindle-shaped morphology, which allows the cells to align according to the structural and functional requirements of the tissue.

These cells also have the ability to contract or exert force in response to stimuli, which is accompanied by massive reorganization and adaptation of the actin cytoskeleton.[54] During mouse cortical development, Hsf2 deficiency leads to neuronal mispositioning through an impaired expression of the actin-bundling protein p35.[25] Silencing of HSF2 disturbs the actin signaling pathway and enhances invasiveness of human prostate cancer PC-3 cells,[55] whereas reduced HSF-1 activity in *Caenorhabditis elegans* results in destabilization of the actin cytoskeleton.[56,57] Since smooth muscle cells, endothelial cells, and myoepithelial cells displayed also cytoplasmic HSF1, it is possible that the presence of HSF1 and HSF2 refers to the role of HSFs in monitoring the cytoskeletal integrity. In striated cardiomyocytes, HSF1 localizes in sarcomeres and is linked to the expression of the co-chaperone BAG3 (BCL-2-associated athanogen).[58] Thereby, it would be interesting to examine if the disruption of cytoskeletal integrity induces HSF1 and/or HSF2 binding at their chaperone targets.

Yet another intriguing common denominator of smooth muscle cells, endothelial cells, and myoepithelial cells is their phenotypic plasticity, i.e., their ability to undergo phenotypic changes in response to physiological cues. In the vasculature, the smooth muscle cells switch between the contractile and synthetic phenotypes upon injuries,[59] while endothelial cells acquire angiogenic or inflammatory phenotypes according to the microenvironment.[60] Also, the morphology of myoepithelial cells depends on mechanical stimuli.[61] Phenotypic plasticity is driven by transcriptional reprogramming, but the molecular details are not fully elucidated. Both HSF1 and HSF2 have been linked with cancer-associated epithelial-mesenchymal transition,[46,55] but whether they regulate cell phenotypic changes also in benign human tissues is unknown. Uncovering the appropriate three-dimensional (3D) model system, with relevant multicellular complexity and adjustable physiological cues, will be of key importance in addressing these highly exciting questions.

HSFs in the formation and maintenance of tissue barriers

The ability to separate the internal and external environments is a fundamental requirement of organismal homeostasis. In the human body, this separation is achieved through cellular barriers mainly composed of epidermal and epithelial cells and their junctional components. A prime example of a cellular barrier is the human skin that restricts water evaporation and pathogen intrusion through powerful cell–cell adhesion contacts composed of adherens junctions, desmosomes, and tight junctions.[62] The transcription factor p63 is essential for epidermal commitment during development,[63] but how the barrier function is regulated at the transcriptional level in adult animals is less clear. We observed nuclear and cytoplasmic localization of HSF1 in basal and surface keratinocytes (Figure 3(A)), suggesting that active HSF1 could promote epidermal homeostasis. Moreover, membrane localization of HSF2 was observed specifically in the surface keratinocytes (Figure 3(A)), which are vital for maintaining proper cell–cell adhesion contacts. Considering that mice deficient in Hsf1 and Hsf2 do not primarily suffer from epidermal insufficiencies,[21,23] it would be important to investigate how these mice recover from, e.g., epidermal wounds or mechanical challenging of the epidermis. The blood-bile barrier refers to a structure within the liver that separates sinusoidal blood from the canalicular bile and thereby protects the hepatocytes from bile toxicities.[33] Tight junctions are the predominant connections in the blood-bile barrier, albeit adherens junctions, desmosomes, and gap junctions have also been described. In our liver samples, HSF2 localized at the canaliculi with a pattern highly similar to the expression pattern of tight junction protein ZO-1 (HPA, ID1846). ZO-1 functions as a scaffolding protein linking junctions with the actin cytoskeleton.[64] Although these findings are correlative, they propose that HSF2 could colocalize with ZO-1 at the blood-bile barrier.

Finally, perhaps the most exciting of all internal barriers is the urothelium, which has a remarkable capacity to withstand a variety of different stress conditions, including osmotic stress, mechanical stress, hydrostatic stress, toxic substances, and microbes.[34] Unlike other mucosal barriers, such as the gastrointestinal epithelium that balance between forming a barrier and allowing selective transport, the urothelium is virtually impermeable. This impermeability is provided by a single layer of apical umbrella cells that have a striking ability to shift in size according to the amount of urine in the bladder. Umbrella cells have an extremely high expression of adherens junction and tight junction proteins that seal the cells together.[34] Unlike HSF1 localized in the nucleus in nearly all studied cell types, HSF2 displayed nuclear localization in only a few cell types, including the urothelial umbrella cells. We hypothesize that the impermeable nature of the urothelium necessitates the constant activation of HSF2 to enable the fully functional barrier capacity.

HSFs in organismal thermoregulation

Sweating and vasodilation are the primary thermoregulatory responses to increased body temperature. Elevation of internal or skin temperature activates afferent neural signals that are integrated with the hypothalamus, the core orchestrator of human thermoregulation.[65] Efferent signaling controls thermal

effector organs, including the sweat glands and the skin vasculature.[66] In our samples, we detected prominent HSF1 and HSF2 levels in secretory cells and myoepithelial cells of sweat glands (Figure 3(B)). In the sweat glands, the luminal secretory cells are responsible for producing the primary sweat, while the myoepithelial cells provide structural support against the hydrostatic pressure and generate the contractile force facilitating sweat expulsion.[29,67] Both the secretion of sweat by the secretory cells and the contraction of the myoepithelial cells are stimulated by sympathetic postganglionic neurons, which release acetylcholine upon elevated temperatures.[29] Analogously to the non-cell autonomous activation of HSF1 in response to neuroendocrine signaling in rat adrenal tissue,[68] the neuronal control of secretory and myoepithelial cells could activate HSFs to ensure the sweat secretion and maintenance of cytoskeletal proteostasis during sweat-expulsing contraction.

In the context of inflammation, the hypothalamic set point is temporarily raised, which enables the increase in body temperature above normal and results in fever. Fever has multiple effects on the human body, such as increased lymphocyte trafficking through HEVs of lymph nodes.[69] Lymphocyte trafficking is accompanied by reorganization of the endothelial actin cytoskeleton, which supports lymphocyte transmigration.[70] In our lymph node samples, HSF1 and HSF2 were expressed in the endothelial cells of HEVs (Figure 9(B)). Considering that HSF2, which has no major impact in acute heat stress, is significantly activated in febrile-range temperatures[12] and that HSF1 and HSF2 gain transcriptional activities in stressed endothelial cells,[15] it would be interesting to elucidate the role of HSF1 and HSF2 in lymphocyte trafficking and endothelial response to febrile-range thermal stress. In general, further investigations in multicellular tissue models could reveal the molecular determinants of HSFs in organismal thermoregulation.

Conclusion

Among human HSFs, HSF1 has been established as a crucial transcription factor for HSP expression and cell survival during protein-damaging stress. Although HSF2 is not required for the stress-inducible expression of HSPs, it contributes to the regulation of cell differentiation and organ development. Nevertheless, the exact role of HSF2 in human physiology has remained enigmatic. Previous studies have mainly relied on cell culture models that do not allow the establishment of multidimensional cell–cell and cell–matrix contacts reflecting tissue integrity. Our findings strongly suggest that HSF2 is important, specifically in multicellular tissue homeostasis. Therefore, future studies focusing on HSF2 should employ model systems that can more closely mimic the complex signaling network of tissues with variable cell types and extracellular matrix components. Albeit we specifically focused on tissues with benign morphology, all samples were collected from patients with an underlying pathological state. Therefore, it would be important to investigate, whether pathological progression in a distant site can cause alterations in the expression and localization of HSF1 and HSF2 in another tissue location. Moreover, the development of new tools is warranted for the identification of post-translationally modified HSFs and distinct HSF isoforms. These technical advancements would enable the characterization of the specific functions of different HSF populations in human tissues. By using a broad selection of human samples, this work expands the biological landscape of HSF1 and HSF2 and thus creates a foundation for the identification of hidden roles of HSF1 and HSF2 in physiological proteostasis. Despite our comprehensive examination, there are still other important tissues to be investigated, such as adipose tissue, bone marrow, CNS, ovaries, and the placenta. Identification of the protein interaction partners of HSF1 and HSF2 in distinct subcellular compartments will reveal novel upstream regulatory mechanisms controlling HSFs. The ultimate goal in understanding HSF biology is to translate the tissue expression patterns of HSFs to transcriptional programs at single-cell resolution.

Materials and methods

Tissue samples

A total of 81 FFPE tissue samples from 71 individuals were used for hematoxylin and eosin (HE) and immunohistochemical stainings (Figure 1). The FFPE tissues and related histopathological data were retrieved from the Biobank of Eastern Finland (BBEF, Kuopio, Finland). Only samples with benign tissue morphology were approved for the study. The samples were pre-selected in the BBEF, and the confirmation of the benign morphology was performed by the two pathologists included in this work (O.J. and R.S.). The tissue material provided by the BBEF originates from the archival tissue collection of Kuopio University Hospital. The colon samples used for immunoblotting (Figure 2(B)) and the skin samples (Figure 3) were obtained from the archival tissue collection of Lapland Central Hospital (LSHP85/2022). All samples were collected in surgical operations conducted as a part of normal diagnostic protocols of the patients. The pathology laboratory responsible for primary tissue

handling and processing in Kuopio University Hospital is a testing laboratory No. T343 accredited by FINAS Finnish Accreditation Service, accreditation requirement SFS-EN ISO15189:2013. The pathology laboratory responsible for primary tissue handling in Lapland Central Hospital is a testing laboratory No. T349 accredited by FINAS Finnish Accreditation Service, accreditation requirement SFS-EN ISO15189:2013. A project-specific consent from the patients was not required as The Finnish Biobank Act provides the legal basis for using patient samples for research purposes. The Scientific Committee of the BBEF provided the approval for using the BBEF material for the study.

HE staining

For HE staining, 5 μm FFPE sections were deparaffinized, rehydrated (xylene 3 × 5 min, absolute ethanol (EtOH) 2 × 2 min, 96% EtOH 2 × 2 min), and washed with dH_2O for 30 s. The sections were incubated in Delafield's hematoxylin (Hematoxylin monohydrate [Merck]; Supelco Aluminium potassium sulfate dodecahydrate [Merck]; AnalaR NORMAPUR ACS Glycerine [VWR International]) for 9 min and 30 s, and washed with running tap water for 5 min. Excess staining was removed with 1% HCl in 70% EtOH for 4 s and running tap water for 5 min. After that, the sections were incubated in 1% eosin (Eosin Y GURR, VWR BDH Chemicals) for 30 s, dehydrated, cleared (96% EtOH 2 × 2 min, absolute EtOH 2 × 2, xylene 2 × 3 and 5 min), and mounted with DPX mounting medium (Merck KGaA).

Immunohistochemistry

FFPE tissues were cut into 4 μm sequential sections, deparaffinized, and rehydrated. For HSF1 and HSF2 stainings, the antigen retrieval was performed in a microwave oven in 0.01 M citrate buffer (pH 6.0). The slides were first heated at 800 W until boiling (7 min and 30 s) and then further boiled for 5 min and 30 s. Prior to the final boiling, more buffer was added if required. After boiling, the sections were incubated in the citrate buffer for another 20 min and washed with phosphate-buffered saline (PBS) for 2 × 5 min. For SMA and CK stainings, the antigen retrieval was performed in a microwave oven in 5 mM ethylenediaminetetraacetic acid (EDTA) buffer (pH 8.0) (SMA) or 10 mM TRIS, 1 mM EDTA (pH 9.0) (CK). The slides were first heated at 800 W until boiling (7 min and 30 s) and then further boiled for 5 min and 30 s. After boiling, the sections were incubated in 5 mM EDTA buffer (SMA) or 10 mM TRIS, 1 mM EDTA (CK) for another 20 min, and washed with PBS for 2 × 5 min. Endogenous peroxidase activity was blocked with 5% hydrogen peroxide for 5 min, and the sections were washed with dH_2O for 2 × 3 min and PBS for 2 × 5 min. For HSF1 and HSF2 stainings, the sections were blocked with 1.5% normal goat serum (VECTASTAIN Elite ABC, Peroxidase Rabbit IgG kit, Vector Laboratories) in PBS for 20 min at room temperature. For SMA and CK stainings, the sections were blocked with 1.5% normal horse serum (VECTASTAIN Elite ABC, Peroxidase Mouse IgG kit, Vector Laboratories) in PBS for 20 min at room temperature.

The following primary antibodies were used: rabbit polyclonal anti-human HSF2 (HPA031455, Sigma-Aldrich), rabbit polyclonal anti-human HSF1 (PA3-017, Invitrogen/Thermo Fisher Scientific), mouse monoclonal anti-human SMA (M0851, clone 1A4, Dako), and mouse monoclonal anti-human CK (M3515, clone AE1/AE3, Dako). The antibodies were used as follows: 1:500 dilution of anti-HSF1 in 1.5% normal goat serum in PBS, 1:100 dilution of anti-HSF2 in 1.5% normal goat serum in PBS, 1:200 dilution of anti-SMA in 1.5% normal horse serum in PBS, and 1:150 dilution of anti-CK in 1.5% normal horse serum in PBS. Sections were incubated in primary antibodies overnight at 4 °C. Negative control sections were incubated in 1.5% normal goat or horse serum in PBS overnight at 4 °C.

The tissue sections on slides were washed with PBS for 2 × 5 min prior to 30 min incubation with biotinylated secondary antibodies (anti-rabbit goat IgG or anti-mouse horse IgG; VECTASTAIN Elite ABC kits) at room temperature. After that, the tissue sections were washed with PBS for 2 × 5 min, incubated for 40 min in preformed avidin-biotinylated peroxidase complex (VECTASTAIN Elite ABC kits), and washed for 2 × 5 min with PBS. For the visualization, diaminobenzidine tetrahydrochloride substrate (Sigma-Aldrich) was used. The tissue sections were counterstained with Mayer's hematoxylin, washed, dehydrated, cleared, and mounted with DPX new mounting medium (Merck KGaA).

For the analysis, the stained sections were scanned using Nanozoomer XR digital slide scanner (Hamamatsu Photonics K.K., Hamamatsu City, Japan) at 40× provided by the BBEF. Images were captured with NDP.view 2 software (Hamamatsu Photonics K.K).

Scoring and evaluation

The cell-type specific expression and localization patterns of HSF1 and HSF2 were evaluated by two independent pathologists (O.J. and R.S.) who were blinded to the scores given by the other pathologist. Following the evaluation, a consensus score was generated for samples with differing primary scores. The intensity of the immuno-signals was scored semi-quantitatively as 0 (negative), 1 (weak), 2 (moderate), and 3 (strong). The staining intensity was evaluated separately in the nucleus and in the cytoplasm.

Protein extraction from FFPE tissue blocks

The proteins were isolated from FFPE colon muscularis propria and mucosal epithelia using the Qproteome FFPE Tissue Kit (37623, QIAGEN) according to the manufacturer's instructions. Briefly, tissue sections were sliced directly from the block and deparaffinized using xylene, followed by repeated washes using EtOH. The proteins were extracted from the remaining tissue pellet by first lysing the cells with Buffer EXB supplemented with β-mercaptoethanol, followed by incubation at a high temperature to ensure the lysis. Finally, the suspension was centrifuged for 15 min at 14,000 g at 4 °C. The supernatant containing the extracted proteins was transferred into a new tube. The protein concentration was measured using the Pierce BCA Protein Assay Kit (23225, Thermo Scientific).

Immunoblotting

Human osteosarcoma U2OS wild-type, *HSF1* knock-out, and *HSF2* knock-out cells have been previously described.[14,47] The cells were cultured in Dulbeccos´s Modified Eagle´s Medium (Sigma Aldrich), supplemented with 10% fetal calf serum, 2 mM L-glutamine (BioWest), and 100 µg/mL penicillin-streptomycin (BioWest) and grown in 5% CO_2 at 37 °C. For immunoblotting, cells were washed in cold PBS (BioWest), after which they were lysed and boiled in 3× Laemmli lysis buffer (30% glycerol, 3% sodium dodecyl sulfate SDS, 187.5 mM TRIS-HCl, 0.015% bromophenol blue, 3% β-mercaptoethanol). Cell samples and the protein samples extracted from tissues were resolved on a 7.5% Mini-PROTEAN Precast Gel (BioRad) and transferred onto a nitrocellulose membrane (Amersham Protran). For detecting HSF2, the membranes were boiled in MQ-H_2O for 20 min and blocked with 5% milk-0.3%-PBS-Tween20. The following antibodies were used for immunoblotting with a 1:1000 dilution: anti-HSF2 (HPA031455, Sigma-Aldrich), anti-HSF1 (ADI-SPA-901, Enzo Life Sciences), and anti-β-Tubulin (T8328, Sigma-Aldrich). Horseradish peroxidase-conjugated secondary antibodies were purchased from Promega and GE Healthcare and used with a 1:10,000 dilution.

Data availability statement No data was used for the research described in the article.

Declarations of interest The authors declare no competing interests.

Acknowledgments Helena Kemiläinen, Aija Kekkonen, Tiina Pirinen, and Ella Ikonen are acknowledged for their expert technical assistance. The authors thank BioBank of Eastern Finland for excellent service and help. Eva Henriksson, Pia Roos-Mattjus, and Malin Åkerfelt are acknowledged for their helpful expert comments on the manuscript. This work has been supported by the Research Council of Finland (L.S.), Sigrid Jusélius Foundation (L.S.), Cancer Foundation Finland (L.S., J.M.H.), Jane and Aatos Erkko Foundation (L.S.), Åbo Akademi University (J.C.P., L.S.), and Lapland hospital district research grant (J.J.). The figures were created with BioRender.com.

References

1. Pessa JC, Joutsen J, Sistonen L. Transcriptional reprogramming at the intersection of the heat shock response and proteostasis. *Mol Cell*. 2023;84:80–93. https://doi.org/10.1016/j.molcel.2023.11.024
2. Gomez-Pastor R, Burchfiel ET, Thiele DJ. Regulation of heat shock transcription factors and their roles in physiology and disease. *Nat Rev Mol Cell Biol*. 2018;19:4–19. https://doi.org/10.1038/nrm.2017.73
3. Joutsen J, Sistonen L. Tailoring of proteostasis networks with heat shock factors. *Cold Spring Harb Perspect Biol*. 2019;11:a034066
. https://doi.org/10.1101/cshperspect.a034066
4. Hartl FU, Bracher A, Hayer-Hartl M. Molecular chaperones in protein folding and proteostasis. *Nature*. 2011;475:324–332. https://doi.org/10.1038/nature10317
5. Roos-Mattjus P, Sistonen L. Interplay between mammalian heat shock factors 1 and 2 in physiology and pathology. *FEBS J*. 2022;289:7710–7725. https://doi.org/10.1111/febs.16178
6. Mendillo ML, Santagata S, Koeva M, et al. HSF1 drives a transcriptional program distinct from heat shock to support highly malignant human cancers. *Cell*. 2012;150:549–562. https://doi.org/10.1016/j.cell.2012.06.031
7. Riva L, Koeva M, Yildirim F, et al. E. Franekel, Poly-glutamine expanded huntingtin dramatically alters the genome wide binding of HSF1. *J Huntingtons Dis*. 2012;1:33–45. https://doi.org/10.3233/JHD-2012-120020
8. Scherz-Shouval R, Santagata S, Mendillo ML, et al. The reprogramming of tumor stroma by HSF1 is a potent enabler of malignancy. *Cell*. 2014;158:564–578. https://doi.org/10.1016/j.cell.2014.05.045
9. Jacobs C, Shah S, Lu WC, et al. HSF1 inhibits antitumor immune activity in breast cancer by suppressing CCL5 to block CD8+ T cell recruitment. *Cancer Res*. 2024;84:276–290. https://doi.org/10.1158/0008-5472.CAN-23-0902
10. Sistonen L, Sarge KD, Phillips B, et al. Activation of heat shock factor 2 during hemin-induced differentiation of human erythroleukemia cells. *Mol Cell Biol*. 1992;12:4104–4111. https://doi.org/10.1128/mcb.12.9.4104-4111.1992
11. Rallu M, Loones M, Lallemand Y, et al. Function and regulation of heat shock factor 2 during mouse embryogenesis. *Proc Natl Acad Sci USA*. 1997;94:2392–2397. https://doi.org/10.1073/pnas.94.6.2392
12. Shinkawa T, Tan K, Fujimoto M, et al. Heat shock factor 2 is required for maintaining proteostasis against febrile-range thermal stress and polyglutamine aggregation. *Mol Biol Cell*. 2011;22:3571–3583. https://doi.org/10.1091/mbc.E11-04-0330

13. El Fatimy R, Miozzo F, Le Mouel A, et al. Heat shock factor 2 is a stress-responsive mediator of neuronal migration defects in models of fetal alcohol syndrome. *EMBO Mol Med.* 2014;6:1043–1061. https://doi.org/10.15252/emmm.201303311
14. Joutsen J, Da Silva AJ, Luoto JC, et al. Heat shock factor 2 protects against proteotoxicity by maintaining cell-cell adhesion. *Cell Rep.* 2020;30:583–597. https://doi.org/10.1016/j.celrep.2019.12.037
15. Rossi A, Riccio A, Coccia M, et al. The proteasome inhibitor bortezomib is a potent inducer of zinc finger an1-type domain 2A gene expression: role of heat shock factor 1 (HSF1) - heat shock factor 2 (HSF2) heterocomplexes. *J Biol Chem.* 2014;289:12705–12715. https://doi.org/10.1074/jbc.M113.513242
16. Fiorenza MT, Farkas T, Dissing M, et al. Complex expression of murine heat shock transcription factors. *Nucleic Acids Res.* 1995;23:467–474. https://doi.org/10.1093/nar/23.3.467
17. Sarge KD, Park-Sarge OK, Kirby JD, et al. Expression of heat shock factor 2 in mouse testis: potential role as a regulator of heat-shock protein gene expression during spermatogenesis. *Biol Reprod.* 1994;50:1334–1343. https://doi.org/10.1095/biolreprod50.6.1334
18. Åkerfelt M, Vihervaara A, Laiho A, et al. Heat shock transcription factor 1 localizes to sex chromatin during meiotic repression. *J Biol Chem.* 2010;285:34469–34476. https://doi.org/10.1074/jbc.M110.157552
19. Metchat A, Åkerfelt M, Biercamp C, et al. Mammalian heat shock factor 1 is essential for oocyte meiosis and directly regulates Hsp90α expression. *J Biol Chem.* 2009;284:9521–9528. https://doi.org/10.1074/jbc.M808819200
20. Salmand PA, Jungas T, Fernandez M, et al. Mouse Heat-Shock Factor 1 (HSF1) Is involved in testicular response to genotoxic stress induced by doxorubicin 1. *Biol Reprod.* 2008;79:1092–1101. https://doi.org/10.1095/biolreprod.108.070334
21. Xiao X, Zuo X, Davis AA, et al. HSF1 is required for extra-embryonic development, postnatal growth and protection during inflammatory responses in mice. *EMBO.* 1999;18:5943–5952. https://doi.org/10.1093/emboj/18.21.5943
22. Wang G, Zhang J, Moskophidis D, Mivechi NF. Targeted disruption of the heat shock transcription factor (hsf)-2 gene results in increased embryonic lethality, neuronal defects, and reduced spermatogenesis. *Genesis.* 2003;36:48–61. https://doi.org/10.1002/gene.10200
23. Kallio M, Chang Y, Manuel M, et al. Brain abnormalities, defective meiotic chromosome synapsis and female subfertility in HSF2 null mice. *EMBO J.* 2002;21:2591–2601. https://doi.org/10.1093/emboj/21.11.2591
24. Åkerfelt M, Henriksson E, Laiho A, et al. Promoter ChIP-chip analysis in mouse testis reveals Y chromosome occupancy by HSF2. *Proc Natl Acad Sci.* 2008;105:11224–11229. https://doi.org/10.1073/pnas.0800620105
25. Chang Y, Östling P, Åkerfelt M, et al. Role of heat-shock factor 2 in cerebral cortex formation and as a regulatorof p35 expression. *Genes Dev.* 2006;20:836–847. https://doi.org/10.1101/gad.366906
26. Wang G, Ying Z, Jin X, et al. Essential requirement for both hsf1 and hsf2 transcriptional activity in spermatogenesis and male fertility. *Genesis.* 2004;38:66–80. https://doi.org/10.1002/gene.20005
27. Fiorenza MT, Farkas T, Dissing M, et al. Complex expression of murine heat shock transcription factors. *Nucleic Acids Res.* 1995;23:467–474. https://doi.org/10.1093/nar/23.3.467
28. Santagata S, Hu R, Lin NU, et al. High levels of nuclear heat-shock factor 1 (HSF1) are associated with poor prognosis in breast cancer. *Proc Natl Acad Sci USA.* 2011;108:18378–18383. https://doi.org/10.1073/pnas.1115031108
29. Baker LB. Physiology of sweat gland function: the roles of sweating and sweat composition in human health. *Temperature.* 2019;6:211–259. https://doi.org/10.1080/23328940.2019.1632145
30. de Thonel A, Ahlskog JK, Daupin K, et al. CBP-HSF2 structural and functional interplay in Rubinstein-Taybi neurodevelopmental disorder. *Nat Commun.* 2022;13:7002. https://doi.org/10.1038/s41467-022-34476-2
31. Bosco D, Armanet M, Morel P, et al. Unique arrangement of α- and β-cells in human islets of Langerhans. *Diabetes.* 2010;59:1202–1210. https://doi.org/10.2337/db09-1177
32. Choudhury A, Ratna A, Lim A, et al. Loss of heat shock factor 1 promotes hepatic stellate cell activation and drives liver fibrosis. *Hepatol Commun.* 2022;6:2781–2797. https://doi.org/10.1002/hep4.2058
33. Pradhan-Sundd T, Monga SP. Blood-bile barrier: morphology, regulation, and pathophysiology. *Gene Expr J Liver Res.* 2019;19:69–87. https://doi.org/10.3727/105221619×15469715711907
34. Jafari NV, Rohn JL. The urothelium: a multi-faceted barrier against a harsh environment. *Mucosal Immunol.* 2022;15:1127–1142. https://doi.org/10.1038/s41385-022-00565-0
35. Åkerfelt M, Morimoto RI, Sistonen L. Heat shock factors: integrators of cell stress, development and lifespan. *Nat Rev Mol Cell Biol.* 2010;11:545–555. https://doi.org/10.1038/nrm2938
36. Alastalo TP, Lönnström M, Leppä S, et al. Stage-specific expression and cellular localization of the heat shock factor 2 isoforms in the rat seminiferous epithelium. *Exp Cell Res.* 1998;240:16–27. https://doi.org/10.1006/excr.1997.3926
37. Izu H, Inouye S, Fujimoto M, et al. Heat shock transcription factor 1 is involved in quality-control mechanisms in male germ cells. *Biol Reprod.* 2004;70:18–24. https://doi.org/10.1095/biolreprod.103.020065
38. Sandqvist A, Björk JK, Åkerfelt M, et al. Heterotrimerization of Heat-Shock Factors 1 and 2 provides a transcriptional switch in response to distinct stimuli. *Mol Biol Cell.* 2009;20:1340–1347. https://doi.org/10.1091/mbc.E08
39. Korfanty J, Stokowy T, Widlak P, et al. Crosstalk between HSF1 and HSF2 during the heat shock response in mouse testes. *Int J Biochem Cell Biol.* 2014;57:76–83. https://doi.org/10.1016/j.biocel.2014.10.006
40. Dong B, Jaeger AM, Thiele DJ. Inhibiting Heat Shock Factor 1 in cancer: a unique therapeutic opportunity. *Trends Pharmacol Sci.* 2019;40:986–1005. https://doi.org/10.1016/j.tips.2019.10.008
41. Kim H, Gomez-Pastor R. HSF1 and its role in Huntington′s disease pathology. *Adv Exp Med Biol.* 2023;1410:35–95. https://doi.org/10.1007/5584_2022_742
42. Kmiecik SW, Mayer MP. Molecular mechanisms of heat shock factor 1 regulation. *Trends Biochem Sci.* 2022;47:218–234. https://doi.org/10.1016/j.tibs.2021.10.004
43. Mathew A, Morimoto RI. Role of the heat-shock response in the life and death of proteins. *Ann N Y Acad Sci.* 1998;851:99–111. https://doi.org/10.1111/j.1749-6632.1998.tb08982.x
44. Sistonen L, Sarge KD, Morimoto RI. Human heat shock factors 1 and 2 are differentially activated and can synergistically induce hsp70 gene transcription. *Mol Cell Biol.* 1994;14:2087–2099. https://doi.org/10.1128/mcb.14.3.2087-2099.1994
45. Carpenter RL, Gökmen-Polar Y. HSF1 as a cancer biomarker and therapeutic target. *Curr Cancer Drug Targets.* 2018;19:515–524. https://doi.org/10.2174/1568009618666181018162117
46. Vydra N, Toma-Jonik A, Janus P, et al. An increase in HSF1 expression directs human mammary epithelial cells toward a mesenchymal phenotype. *Cancers.* 2023;15:4965. https://doi.org/10.3390/cancers15204965

47. Pesonen L, Svartsjö S, Bäck V, et al. Gambogic acid and gambogenic acid induce a thiol-dependent heat shock response and disrupt the interaction between HSP90 and HSF1 or HSF2. *Cell Stress Chaperones.* 2021;26:819–833. https://doi.org/10.1007/s12192-021-01222-4
48. Díaz-Díaz C, Baonza G, Martín-Belmonte F. The vertebrate epithelial apical junctional complex: dynamic interplay between Rho GTPase activity and cell polarization processes. *Biochim Biophys Acta - Biomembr.* 2020;1862:183398. https://doi.org/10.1016/j.bbamem.2020.183398
49. Zhao G, Qiu Y, Zhang HM, Yang D. Intercalated discs: cellular adhesion and signaling in heart health and diseases. *Heart Fail Rev.* 2019;24:115–132. https://doi.org/10.1007/s10741-018-9743-7
50. Lessey LR, Robinson SC, Chaudhary R, Daniel JM. Adherens junction proteins on the move - from the membrane to the nucleus in intestinal diseases. *Front Cell Dev Biol.* 2022;10:998373. https://doi.org/10.3389/fcell.2022.998373
51. Vihervaara A, Sergelius C, Vasara J, et al. Transcriptional response to stress in the dynamic chromatin environment of cycling and mitotic cells. *Proc Natl Acad Sci USA.* 2013;110:E3388–E3397. https://doi.org/10.1073/pnas.1305275110
52. Björk JK, Sandqvist A, Elsing AN, et al. miR-18, a member of Oncomir-1, targets heat shock transcription factor 2 in spermatogenesis. *Development.* 2010;137:3177–3184. https://doi.org/10.1242/dev.050955
53. Ahlskog JK, Björk JK, Elsing AN, et al. Anaphase-promoting complex/cyclosome participates in the acute response to protein-damaging stress. *Mol Cell Biol.* 2010;30:5608–56020. https://doi.org/10.1128/MCB.01506-09
54. Clarke DN, Martin AC. Actin-based force generation and cell adhesion in tissue morphogenesis. *Curr Biol.* 2021;31:R667–R680. https://doi.org/10.1016/j.cub.2021.03.031
55. Björk JK, Åkerfelt M, Joutsen J, et al. Heat-shock factor 2 is a suppressor of prostate cancer invasion. *Oncogene.* 2016;35:1770–1784. https://doi.org/10.1038/onc.2015.241
56. Baird NA, Douglas PM, Simic MS, et al. HSF-1-mediated cytoskeletal integrity determines thermotolerance and life span. *Science.* 2014;346:360–363. https://doi.org/10.1126/science.1253168
57. Watterson A, Arneaud SLB, Wajahat N, et al. Loss of heat shock factor initiates intracellular lipid surveillance by actin destabilization. *Cell Rep.* 2022;41:111493. https://doi.org/10.1016/j.celrep.2022.111493
58. Martin TG, Tawfik S, Moravec CS, et al. BAG3 expression and sarcomere localization in the human heart are linked to HSF-1 and are differentially affected by sex and disease. *Am J Physiol Heart Circ Physiol.* 2021;320:H2339–H2350. https://doi.org/10.1152/AJPHEART.00419.2020
59. Miano JM, Fisher EA, Majesky MW. Fate and state of vascular smooth muscle cells in atherosclerosis. *Circulation.* 2021;143:2110–2116. https://doi.org/10.1161/CIRCULATIONAHA.120.049922
60. Pilard M, Ollivier EL, Gourdou-Latyszenok V, et al. Endothelial cell phenotype, a major determinant of venous thrombo-inflammation. *Front Cardiovasc Med.* 2022;9:864735. https://doi.org/10.3389/fcvm.2022.864735
61. Hayward MK, Allen MD, Gomm JJ, et al. Mechanostimulation of breast myoepithelial cells induces functional changes associated with DCIS progression to invasion. *NPJ Breast Cancer.* 2022;8:109. https://doi.org/10.1038/s41523-022-00464-4
62. Sumigray KD, Lechler T. Cell adhesion in epidermal development and barrier formation. *Curr Top Dev Biol.* 2015;112:383–414. https://doi.org/10.1016/bs.ctdb.2014.11.027
63. Mills AA, Wang XJ, Zheng B, et al. P63 is a P53 homologue required for limb and epidermal morphogenesis. *Nature.* 1999;398:708–713. https://doi.org/10.1038/19531
64. Van Itallie CM, Fanning AS, Bridges A, Anderson JM. ZO-1 stabilizes the tight junction solute barrier through coupling to the perijuncitonal cytoskeleton. *Mol Biol Cell.* 2009;20:3930–3940. https://doi.org/10.1091/mbc.E09
65. Zhao ZD, Yang WZ, Gao C, et al. A hypothalamic circuit that controls body temperature. *Proc Natl Acad Sci USA.* 2017;114:2042–2047. https://doi.org/10.1073/pnas.1616255114
66. Smith CJ, Johnson JM. Responses to hyperthermia. Optimizing heat dissipation by convection and evaporation: neural control of skin blood flow and sweating in humans. *Auton Neurosci Basic Clin.* 2016;196:25–36. https://doi.org/10.1016/j.autneu.2016.01.002
67. Cui C-Y, Schlessinger D. Eccrine sweat gland development and sweat secretion. *Exp Dermatol.* 2015;24:644–650. https://doi.org/10.1111/exd.12773
68. Fawcett TW, Sylvester SL, Sarge KD, et al. Effects of neurohormonal stress and aging on the activation of mammalian heat shock factor 1. *J Biol Chem.* 1994;269:32272–32278. https://doi.org/10.1016/s0021-9258(18)31631-4
69. Chen Q, Fisher DT, Clancy KA, et al. Fever-range thermal stress promotes lymphocyte trafficking across high endothelial venules via an interleukin 6 trans-signaling mechanism. *Nat Immunol.* 2006;7:1299–1308. https://doi.org/10.1038/ni1406
70. Yan SLS, Hwang IY, Kamenyeva O, Kehrl JH. In vivo f-actin filament organization during lymphocyte transendothelial and interstitial migration revealed by intravital microscopy. *iScience.* 2019;16:283–297. https://doi.org/10.1016/j.isci.2019.05.040